CONFIDENTIAL

(NASA-CR-117566) STATIC STABILITY AND FORCE CHARACTERISTICS OF A 0.02-SCALE MODEL OF THE SATURN C-1 LAUNCH VEHICLE WITH APOLLO PAYLOAD FOR THE MACH NUMBER RANGE 0.70 TO 3.50 (North American Aviation, Inc.) 42 p 00/02

N79-76089

Unclas
11408

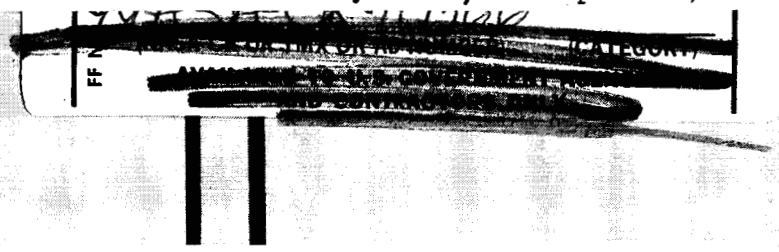

Apollo

CONFIDENTIAL

[redacted]

Z65·11726

This issue replaces and supersedes all previous issues of this report.

Accession No. 19932

SID 62-1391-R-1

STATIC STABILITY AND FORCE CHARACTERISTICS OF A 0.02-SCALE MODEL OF THE SATURN C-1 LAUNCH VEHICLE WITH APOLLO PAYLOAD FOR THE MACH NUMBER RANGE 0.70 TO 3.50

NAS9-150

(U)

#5

ASPO DISTRIBUTION COPY

Destroy when no longer [redacted]

Do not return to ASPO file

Reissued April 1963

CLASSIFICATION CHANGE

To UNCLASSIFIED

By authority of GDS - Fa 11/62

Changed by L. Shirley Date 12/3/62

Classified Document Master Control Station, NASA

Scientific and Technical Information Facility

[redacted]

This document contains information affecting the national defense of the United States within the meaning of the Espionage Laws. Title 18 U.S.C. Section 793 and 794. Its transmission or revelation of its contents in any manner to an unauthorized person is prohibited by law.

NORTH AMERICAN AVIATION, INC.
SPACE and INFORMATION SYSTEMS DIVISION

[redacted]

[redacted]

FOREWORD

The static stability characteristics study of the FSL-1 model was conducted under NASA Apollo Contract NAS9-150.

This report was prepared by F. L. Goebel of the Columbus Division of North American Aviation, Inc.

CONFIDENTIAL

SUMMARY

The static stability and force characteristics of a 0.02-scale model of the Saturn C-1 launch vehicle with Apollo payload were investigated in the launch and launch-abort configurations for the Mach number range 0.70 to 3.50 in Ames Research Center, Unitary Plan Wind Tunnels.

The data indicated no dependency on Reynolds number in the range attainable. The addition of the command module clamp fairing had no appreciable effect on the aerodynamic characteristics. Removal of the launch escape system flow separator had a small but measurable effect on axial force and pitching moment. Removal of the jet reaction controls from the launch-abort configuration affected the flow field in the transonic speed range and thereby affected the aerodynamic characteristics.

Several effects of roll attitude on the aerodynamic characteristics, apparently attributable to the fins, were observed in the subsonic-transonic speed range.

CONTENTS

Section		Page
I	INTRODUCTION	1
II	MODEL AND TESTS	2
	Model	2
	Tests	2
III	RESULTS AND DISCUSSION	5
	Presentation of Results	5
	Effect of Reynolds Number Variation	6
	Effect of Transition Grit	7
	Effect of Clamp Fairing	7
	Effect of Flow Separator	7
	Effect of Jet Reaction Controls	8
	Effect of Roll Attitude	8
	Nonlinearity of Aerodynamic Coefficients	10
IV	CONCLUSIONS	11
V	SYMBOLS	13

CONFIDENTIAL

ILLUSTRATIONS

Figure		Page
1	Test Configurations	15
2	Launch Configuration	16
3	Launch-Abort Configuration	17
4	Variation of Reynolds Number With Mach Number	18
5	Effect of Mach Number on the Aerodynamic Coefficients for the Launch Configuration	19
6	Effect of Mach Number on the Aerodynamic Coefficients for the Launch-Abort Configuration	22
7	Schlieren Photographs of Attached and Separated Flow Fields at Mach Number 1.20	25
8	Effect of Separation of Mach Number 1.20 for Launch-Abort Configuration	26
9	Effect of Launch Escape System Separator on Axial Force and Pitching Moment	27
10	Effect of Roll Attitude on Normal Force Coefficient	28
11	Effect of Roll Attitude on Inclination of Composite Normal Force Coefficient	29
12	Effect of Mach Number of Rolling Moment Coefficient at β = 0 and 6.5 Degrees	30
13	Effect of Mach Number on the Increment of Rolling Moment Coefficient Due to Angle of Attack at β = 6.5	31
14	Effect of Mach Number on Aerodynamic Coefficients at Angles of Attack for the Launch Configuration	32
15	Effect of Mach Number on Aerodynamic Coefficients at Angles of Attack for Launch-Abort Configuration	35

I. INTRODUCTION

Static stability and force characteristics of the Saturn C-1 launch vehicle with the Apollo payload are being investigated with a 0.02-scale model (FSL-1) in the Mach number range from 0.30 to 8.00. This program consists of a series of wind tunnel tests at four facilities: Ames Research Center, Arnold Engineering Development Center, NAA Trisonic, and NAA NACAL. This report presents the analysis of the results of the first series conducted in the Ames Research Center Unitary Plan Wind Tunnels during the period 22 August to 5 September 1962. The basic data and graphs for this first series are presented in the data report.[1]

The purpose of the Ames tests was to investigate the static stability and force characteristics of the launch and launch-abort configurations in the Mach number range from 0.70 to 3.50. The effects of Reynolds number, transition grit, command module clamp fairing, launch escape system flow separator ring, and jet reaction controls on the basic data were also investigated.

[1]Data Report for the Apollo Model (FSL-1 Wind Tunnel Tests in the Ames Unitary Plan Wind Tunnels, 11- by 11-Foot, 9- by 7-Foot, and 8- by 7-Foot. NAA/S&ID SID 62-1143.

II. MODEL AND TESTS

MODEL

The 0.02-scale model consisted of the complete launch configuration (FSL-1) of the Apollo payload with the Saturn C-1 launch vehicle. Provisions were incorporated for removal of the launch escape system flow separator, command module clamp, and jet reaction controls. Furthermore, the launch escape vehicle and a section of the service module were removable for installation of the launch-abort nose. A detailed description of the model is contained in SID 62-805[1]. Sketches of the configurations tested are presented in Figure 1 and photographs of the model are shown in Figures 2 and 3.

TESTS

Axial, normal and side force and pitching, yawing, and rolling moment were measured by a Task 2-inch Mark IX A balance in the 11- by 11-foot and 9- by 7-foot tunnels and by a Task 2-inch Mark III F balance in the 8- by 7-foot tunnel. One static pressure measured in the balance chamber was assumed to be representative of the actual base pressure acting over the base of the model.

The tests conducted are listed in Table 1. The primary configurations were launch ($B_3I_2S_4RC_2T_{20}E_{40}$) and launch-abort ($B_3I_2S_4R$). Limited evaluations were made of the effect of adding the command module clamp and removing the launch escape system flow separator and jet reaction controls, and the effects of Reynolds number and grit were investigated. Transition grit was used for all tests except for two runs with the launch configuration at Mach number 1.55. In the 11- by 11-foot and 9- by 7-foot tunnels, 0.009-inch diameter grit with a density of 900 grains per square inch was used, and 0.014 diameter grit with a density of 900 grains per square inch was used in the 8- by 7-foot tunnel. The grit was applied to a 0.1-inch-wide strip located immediately aft of the escape motor nose cone cylinder junction and to a 0.1-inch-wide strip located 0.1 inch from the leading edges of the large fins.

[1] Test and Model Information for Wind Tunnel Tests of a 0.02-Scale Force Model (FSL-1) of the Apollo in the Ames 14- by 14-Foot, 9- by 7-Foot, and 8- by 7-Foot Wind Tunnels. NAA/S&ID SID 62-805.

In general, data were obtained for an angle-of-attack range from -4 to 20 degrees with reduction to 16 degrees in the Mach number range 1.0 to 2.5. In addition, sideslip runs at $\alpha = 0$ were obtained at Mach numbers 0.70, 1.05, and 1.40 with the launch configuration. Effects of combined sideslip and pitch (or roll attitude) were investigated at eight Mach numbers from 0.70 to 3.50 with the launch configuration and at Mach number 0.95 with the launch-abort configuration. The variation of tunnel Reynolds number with Mach number is presented in Figure 4.

Table 1. Completed Runs of Apollo 0.02-Scale Model Wind Tunnel Test

Facility: Ames Research Center
Model: FSL-1

Configuration	Grit*	β (deg)	P_T (in. Hg)	Run Number: 11- by 11-Foot Tunnel — Mach Number 0.7	0.9	0.95	1.0	1.05	1.1	1.2	1.4	9- by 7-Foot Tunnel — Mach Number 1.55	1.7	2.0	2.5	8- by 7-Foot Tunnel — Mach Number 2.5	3.0	3.5
$B_3I_2S_4RC_2T_{20}E_{40}$	On	0	20								1							
	On	0	30									6	7	8	9	4	3	1
	On	6	30												10			1
	On	0	45	20	18	17	15	13	11	9	3							2
	On	0	45								4							
	On	-3	45								5							
	On	3	45								6							
	On	6	45	21	19		16		12	10	7							
	On	Vary	45	22				14			8			(Yaw Runs at α = 0 deg)				
	On	0	60								2							
	Off	0	15									12						
	Off	0	30									11						
$B_3I_2S_4RC_2T_{20}E_{35}$	On	0	20								24							
	On	0	45	27				26			25							
	On	0	60								23							
$B_3I_2S_4RK_2C_2T_{20}E_{40}$	On	Vary	45	42				41			40	(Yaw Runs at α = 0 deg)						
$B_3I_2S_4R$	On	0	30									2	3	4	5	7	6	5
	On	0	40									1						
	On	0	45	36	35	33	32	31	30	29	28							
	On	6	45			34												
$B_3I_2S_4$	On	0	45					39		38	37							

*Note: 0.009-inch diameter grit used in 11- by 11-foot and 9- by 7-foot tunnels, 900 grains/in.^{2} density
0.014-inch diameter grit used in 8- by 7-foot tunnel, 900 grains/in.^{2} density

III. RESULTS AND DISCUSSION

PRESENTATION OF RESULTS

Summary results of the test data are presented in the form of C_{N_α}, C_{m_α}, X_{cp}/D, C_A, and C_{p_b} versus Mach number for configurations $B_3I_2S_4RC_2T_{20}E_{40}$ (launch) and $B_3I_2S_4R$ (launch-abort). All coefficients presented herein are referenced to command module frontal area, and the reference length is command module maximum diameter, which accounts for the apparent large magnitude of the coefficients. All pitching moment data are referenced to a moment center, based on a representative center of mass, located 3.726 command module diameters forward of the base.

Configuration $B_3I_2S_4RC_2T_{20}E_{40}$

The summary plots for the launch configuration are presented in Figure 5. The transonic peaks in C_{N_α} and C_{m_α} occur near Mach number 0.96 and are characterized by relatively gentle changes in curvature. C_{m_α} is slightly unstable subsonically and slightly stable transonically. From Mach number 1.10 to 3.50, C_{m_α} becomes increasingly unstable in an almost linear manner. The center of pressure varies from about 3.90 diameters forward of the base subsonically to a maximum aft position of about 3.43 diameters at Mach number 0.96. From Mach number 0.96 to 3.50, the center of pressure moves continuously forward to a position of 5.92 diameters.

Comparison of the C_{N_α} data with data obtained in the Chance Vought Aeronautics 4- by 4-foot wind tunnel for a similar configuration shows excellent agreement. The center-of-pressure comparison, however, shows some disagreement at the higher Mach numbers. Over Mach number 2.0, the Chance Vought data indicate a decreased forward shift. The model tested at Chance Vought did not incorporate the launch escape system flow separator and had a shortened I_2S_4 section. These differences may account for the center-of-pressure shift.

The total axial force reaches a transonic peak, about twice the subsonic level, at Mach number 1.12. With the base drag removed, the transonic to subsonic ratio is slightly less than 2, and the peak occurs at Mach number 1.20. Axial force divergence occurs in the vicinity of Mach number 0.80, and reduction after the transonic peak is very gradual.

Configuration $B_3I_2S_4R$

The summary plots for the launch-abort configuration are presented in Figure 6. The data indicate distinctly different characteristics for separated and attached flow fields surrounding the nose section. Separated flow fields were observed in the subsonic and transonic speed range up to Mach number 1.40; while attached flow was observed over Mach number 1.55. An exception was observed at Mach number 1.20; where attached flow was achieved with the jet reaction controls removed. The effects of separation at $\alpha = \beta = 0$ are increase in C_{N_α}, decrease in C_{m_α}, aft shift in X_{cp}/D, and a decrease in C_A. Although the flow around the nose is not attached at Mach number 1.4 with jet reaction controls installed, the degree of separation does not appear to affect the data appreciably.

The C_{N_α} for the separated range of Mach numbers closely approximates the C_{N_α} for the launch configuration. When attachment occurs, however, C_{N_α} decreases about 10 percent and subsequently decreases at a slightly higher rate with increasing Mach number than the C_{N_α} for the launch configuration. The transonic peaks for C_{N_α} and C_{m_α} occur near Mach number 1.00. Except in the immediate vicinity of force divergence Mach number, C_{m_α} for the launch-abort configuration is slightly more stable than C_{m_α} for the launch configuration. The incremental difference between the two C_{m_α}'s increases with increasing Mach number to about 1.8 but remains approximately constant as Mach number is increased beyond 1.8.

The launch-abort base pressure coefficient variation with Mach number is essentially the same as that obtained for the launch configuration. Curvature changes in the axial force are more abrupt in the vicinity of force divergence (approximately Mach number 0.90) but are smaller in the transonic speed range when compared with the launch configuration. The decrease in axial force associated with flow separation is primarily attributed to the effect of separation on the shock produced by the flare following the I_2S_4 section. Examination of the Schlieren photographs in Figure 7 indicates a more oblique flare shock when the flow is separated. The decreased shock strength results in reduced wave drag for the separated flow. For angles of attack greater than about 8 degrees, the difference disappears in C_A, C_N, and C_m for flow fields initially attached and separated. This variation of the separation effect with α for C_A, C_N, and C_m at Mach number 1.20 is presented in Figure 8.

EFFECT OF REYNOLDS NUMBER VARIATION

An investigation was conducted to determine effect of Reynolds number on the force and moment data and to provide correlation with future

wind tunnel tests. The Reynolds numbers and configurations that were investigated are shown in the following tabulation:

Configuration	Mach No.	RN per foot x 10^{-6}
$B_3I_2S_4RC_2T_{20}E_{40}$	1.40 3.50	2.92, 6.20-6.43, 8.21 1.67, 2.34
$B_3I_2S_4RC_2T_{20}E_{35}$	1.40	2.92, 6.35, 8.19
$B_3I_2S_4R$	1.55	3.97, 4.99

A planned, higher Reynolds number test with configuration $B_3I_2S_4R$ was eliminated when the tunnel operating temperature limits were exceeded. No significant variations or trends attributable to Reynolds number were observed for the configurations and Reynolds numbers tested.

EFFECT OF TRANSITION GRIT

Force and moment data for configuration $B_3I_2S_4RC_2T_{20}E_{40}$ were obtained at Mach number 1.55 with and without transition grit at Reynolds number 3.95×10^6 per foot and without grit at Reynolds number 1.52×10^6 per foot. No definite differences attributable to the grit were observed. It is therefore assumed that the boundary layer was naturally turbulent owing to nose bluntness and escape system structure.

EFFECT OF CLAMP FAIRING

The effect of a clamp fairing between the command module and service module, centered along the top meridian of the model, was investigated by using sideslip runs at $\alpha = 0$ at Mach numbers 0.70, 1.05, and 1.40. No effect of the clamp fairing was detected.

EFFECT OF FLOW SEPARATOR

To evaluate the effect of the launch escape system flow separator, tests were conducted at Mach numbers 0.70, 1.05, and 1.40 with the separator on and off. These effects of the separator are shown in Figure 9. No clear effect of the separator on normal force was observed. The effect of the separator on pitching moment was masked by data scatter except at Mach number 1.40, where the C_m increment due to separator is 0.1 to 0.2 at positive angles of attack. The separator has a measurable effect on axial force coefficient at all three test Mach numbers. At Mach number 0.70, the axial force increment is positive and increases linearly with angle of

attack. At Mach numbers 1.05 and 1.40, the axial force increment is negative at small angles and increases gradually to a very small positive increment at large angles of attack.

EFFECT OF JET REACTION CONTROLS

The effect of removing the jet reaction controls was investigated with the launch-abort configuration, which was presumed to be most sensitive to the controls. These tests were conducted at Mach numbers 1.05, 1.20, and 1.40. No direct effect was observed; however, a flow field change observed at Mach 1.20 may be associated with the jet reaction controls. With the reaction controls installed, the flow is at least partially separated from the nose for all Mach numbers up through 1.20. At Mach number 1.40, the separated layer is considerably reduced in thickness and apparently has no appreciable effect on the aerodynamic forces and moments. For Mach numbers less than 1.05, the flow fields are essentially similar with reaction controls on and off. Schlieren photographs at Mach number 1.05 show no apparent difference except for the weak shocks emanating from the reaction controls. At Mach number 1.20, however, the flow is definitely attached with the reaction controls removed, as may be seen in Figure 7. Although no Schlieren photographs are available for Mach number 1.40 with reaction controls removed, it is presumed that the flow is attached at this velocity also. For the launch-abort configuration, it appears that the reaction controls, critically located near the nose, encourage flow separation in the transonic speed range.

EFFECT OF ROLL ATTITUDE

For a pure body of revolution, the aerodynamic characteristics would be independent of roll attitude. In addition to the nonaxial symmetry of the C-1 booster and the combination of large and small fins, the FSL-1 has certain design asymmetries that could conceivably affect the aerodynamic characteristics. The major design asymmetries include a chilldown duct omitted from the lower left small fin; four equispaced exhaust ducts located 22.5 degrees clockwise from the planes of the large fins; three external ducts on the second stage at 51.5, 141.5 and 308.5 degrees measured clockwise from the upper meridian; and a horizon sensor on the instrumentation module slightly offset to the right on the lower meridian.

The effect of roll attitude was investigated indirectly, since the model had no provisions for varying roll attitude on the sting. Variations in roll attitude were obtained for the launch configuration by conducting pitch runs at approximately 6.5 degrees of sideslip at eight Mach numbers and sideslip runs at $\alpha = 0$ at Mach numbers 0.70, 1.05, and 1.40. In addition, pitch

runs were made at ±3 degrees of sideslip at Mach number 1.40. Variations in roll attitude were obtained for the launch-abort configuration by conducting pitch runs at approximately 6.3 degrees of sideslip at Mach number 0.95.

A comparison of the data from the sideslip runs at $\alpha = 0$ with the data from pitch runs at $\beta = 0$ shows no difference. This result indicates that the asymmetric protuberances have little influence. However, the data show variations in C_N, C_m and therefore X_{cp}/D for the pitch runs at $\beta = 6.5$ degrees. The data were compared on the basis of composite normal force and pitching moment ($\overline{C}_N = \sqrt{C_N^2 + C_Y^2}$, $\overline{C}_m = \sqrt{C_m^2 + C_n^2}$) versus composite angle of attack ($\cos \overline{\alpha} = \cos \alpha \cos \beta$). This approach is equivalent to considering the model being rolled and then pitched. The roll angle ϕ may be computed from α and β by $\tan \phi = \frac{\tan \beta}{\sin \alpha}$.

Figure 10 presents the ratio of the composite normal force coefficient to the normal force coefficient for $\phi = 0$ versus the equivalent roll angle. For the Mach number range 0.70 to 1.20, the data show a uniform sinusoidal-type variation with roll angle for both launch and launch-abort configurations. The data indicate a maximum decrement in the vicinity of $\phi = 45$ degrees with a trend toward another maximum decrement at $\phi = 135$ degrees, although the data only extend to 123 degrees. The pitching moment data (not shown) exhibit similar characteristics although definition is poor because of the magnitude of the pitching moment coefficients in comparison with data scatter.

The reduction in composite normal force coefficient disappears for Mach numbers equal to or greater than 1.40. At these higher Mach numbers, composite normal force is independent of roll attitude. Similarly, the effect of roll attitude on pitching moment essentially disappears at Mach numbers greater than about 1.40.

Another phenomenon uncovered in the yawed attitude is the inclination of the composite normal force with respect to the plane containing the composite angle of attack. Figure 11 illustrates this effect. The inclination appears to be 0 at roll angles of $n\frac{\pi}{4}$ and maximum at angles of $(2n-1)\,\pi/8$, indicating that the inclination is a function of roll orientation of the fins. This phenomenon also disappears at Mach numbers greater than about 1.20.

A small rolling moment existed throughout the Mach number range tested for both launch and launch-abort configurations. At $\alpha = \beta = 0$, the rolling moment coefficient reaches a maximum of -0.125 in the transonic speed range, while at higher speeds it decreases in magnitude and crosses 0 near Mach number 2.8. For $\alpha = 0$, $\beta = 6.5$ degrees, C_ℓ increases approximately +0.02 at supersonic speeds but is unaffected at subsonic speeds.

These small rolling moment coefficients, shown in Figure 12, are presumably the result of design asymmetries and possibly a very small misalignment of one or more of the fins (less than 0.1 degree).

As the angle of attack is increased from 0 in the yawed attitude, the rolling moment shifts toward positive values, see Figure 13. This effect may be explained on the basis of the upper vertical fin being blanketed at positive angles of attack. The resulting loss of fin lift would lead to a positive rolling moment increment.

NONLINEARITY OF AERODYNAMIC COEFFICIENTS

A summary of the effects of angle of attack on C_N, C_m and C_A for Mach numbers 0.70 to 3.50 is presented for the launch and launch-abort configurations in Figures 14 and 15. It is noted that the discontinuities in the launch-abort curves in the vicinity of Mach number 1.2 for $\alpha = \pm 4$ degrees are associated with separation-attachment phenomena previously discussed.

In general, C_N is linear up to at least $\alpha = 4$ degrees. At some angle between 4 and 8 degrees, dependent on Mach number, C_{N_α} starts to increase, indicating a body cross-flow lift increment. Subsonically, at some angle between 12 and 16 degrees, C_{N_α} tends to decrease again toward a value near C_{N_α} for $\alpha = 0$. This reduction may be attributable to a loss of fin lift. For angles of attack less than about 4 degrees, C_N is only slightly dependent on Mach number even in the transonic speed range.

C_m is nonlinear for angles of attack greater than about 2 degrees; however, the variations in C_m for angles up to about 6 degrees are small. For Mach number range 0.8 to 1.4 and α greater than 4 degrees, the variations in C_m with Mach number and α are relatively large. At subsonic speeds, there is a relatively large positive increase in C_m with angles of attack greater than 12 degrees. This is also attributable to a loss in fin lift. As Mach number increases beyond 2.0, the variation of C_m with Mach number tends to decrease.

For the launch configuration, the axial force is minimum in the vicinity of $\alpha = 0$ for all Mach numbers from 0.70 to 3.50. At $\alpha = 8$ and 16 degrees, the C_A's are nearly equal up to about Mach number 1.6. Above Mach number 1.6, C_A for $\alpha = 16$ degrees increases relative to the C_A for $\alpha = 8$ degrees. For the launch-abort configuration with flow field initially separated (Mach numbers 0.70 to 1.4), C_A is minimum in the vicinity of $\alpha = 0$ and C_A for $\alpha = 8$ degrees is slightly larger than C_A for $\alpha = 16$ degrees (Figure 15). With the flow field initially attached and Mach numbers greater than 1.6, C_A is largest at $\alpha = 0$ and decreases as α is increased to 16 degrees. As the Mach number increases beyond 1.6, an inversion of the variation of C_A with α takes place such that at Mach number 3.5, C_A is smallest at $\alpha = 0$ and greatest at $\alpha = 16$ degrees.

IV. CONCLUSIONS

The static stability and force characteristics of the launch and launch-abort configurations of a 0.02-scale model of the Saturn C-1 launch vehicle with Apollo payload have been tested in the Mach number range 0.70 to 3.50. The results of this investigation indicate the following conclusions.

1. For the representative moment center, the launch and launch-abort configurations are slightly unstable in the subsonic speed range, slightly stable in the transonic speed range, and slightly unstable at supersonic speeds. In general, the launch configuration is more unstable than the launch-abort configuration.

2. The launch-abort configuration exhibits a discontinuity in the aerodynamic coefficients in the vicinity of Mach number 1.2 that is associated with separation-attachment phenomena. The flow field about the nose is initially separated at speeds below about Mach number 1.2 and is initially attached at higher speeds.

3. No significant variation of the aerodynamic coefficients was observed in the Reynolds number range attainable during the tests.

4. Application of transition grit to the escape rocket and large fins had no apparent effect on the data, which indicates the flow was naturally turbulent.

5. The addition of the clamp fairing to the launch configuration had no effect on the data.

6. Removal of the launch escape system flow separator had a small but measurable effect on the axial force coefficient at Mach number 0.70, 1.05, and 1.40 and on the pitching moment coefficient at Mach number 1.40.

7. Removal of the jet reaction controls from the launch-abort configuration had no inherent effect on the data; however, removing the controls apparently permitted the flow field to become attached at a lower Mach number.

8. The aerodynamic coefficients were sensitive to roll attitude at Mach numbers less than about 1.40. Variations in the coefficients

are apparently associated with variations in fin lifting capability with roll attitude. A maximum reduction in C_N occurs at roll attitudes of $(2n - 1)\frac{\pi}{4}$. Furthermore, an inclination of the composite normal force vector with respect to the true pitch plane was uncovered and which varied with roll attitude and had maximum magnitude at $\phi = (2n - 1)\frac{\pi}{8}$.

9. A small rolling moment that existed throughout the Mach number range (0.70 to 3.50) for both launch and launch-abort configurations may have been the result of a very small misalignment of one or more of the fins.

V. SYMBOLS

The data are referred to the system of body axes. The coefficients and symbols used herein are defined as follows.

A_b	Model base area (used in computing base axial force) 0.1364 ft^2
C_A	Axial force coefficient (base axial force removed), $(C_{A_{total}} - \Delta C_A)$
$C_{A_{total}}$	Axial force coefficient (including base effects), axial force/qS
ΔC_A	Base axial force coefficient, $- C_{p_b} A_b/S$
C_ℓ	Rolling moment coefficient, rolling moment/qSD
C_m	Pitching moment coefficient about moment center 3.726 D forward of base, pitching moment/qSD
$\overline{C}_m$	Composite pitching moment coefficient, $\overline{C}_m = \sqrt{C_m^2 + C_n^2}$
C_{m_α}	Slope of pitching moment coefficient versus angle of attack, 1/degrees
C_n	Yawing moment coefficient about moment center 3.726 diameters forward of base, yawing moment/qSD
C_N	Normal force coefficient, normal force/qS
$\overline{C}_N$	Composite normal force coefficient, $\overline{C}_N = \sqrt{C_N^2 + C_Y^2}$
C_{N_α}	Slope of normal force coefficient versus angle of attack, 1/degrees
C_{p_b}	Base pressure coefficient $(p_b - p_\infty)/q$
C_Y	Side force coefficient, side force/qS

D	Reference length (command module maximum diameter), 0.2567 ft
M	Free-stream Mach number
n	Any integer
p_b	Model base pressure, lb/ft^2
p_t	Free-stream stagnation pressure, lb/ft^2
p_∞	Free-stream static pressure, lb/ft^2
q	Free-stream dynamic pressure, lb/ft^2
R_N	Free-stream Reynolds number per ft
S	Reference area (based on command module maximum diameter), 0.0517 ft^2
$\frac{X_{cp}}{D}$	Center of pressure location measured in reference diameters from the base, positive forward, $\frac{C_m}{C_N} + \frac{\overline{X}}{D}$
$\overline{X}$	Transfer distance from model base to moment reference center, 3.726 diameters
α	Angle of attack, degrees
$\bar{\alpha}$	Composite angle of attack, $\cos \bar{\alpha} = \cos \alpha \cos \beta$
β	Angle of sideslip, degrees
ϕ	Angle of roll, degrees

The subscript $\alpha = 0$ denotes conditions existing at 0 angle of attack.

CONFIDENTIAL

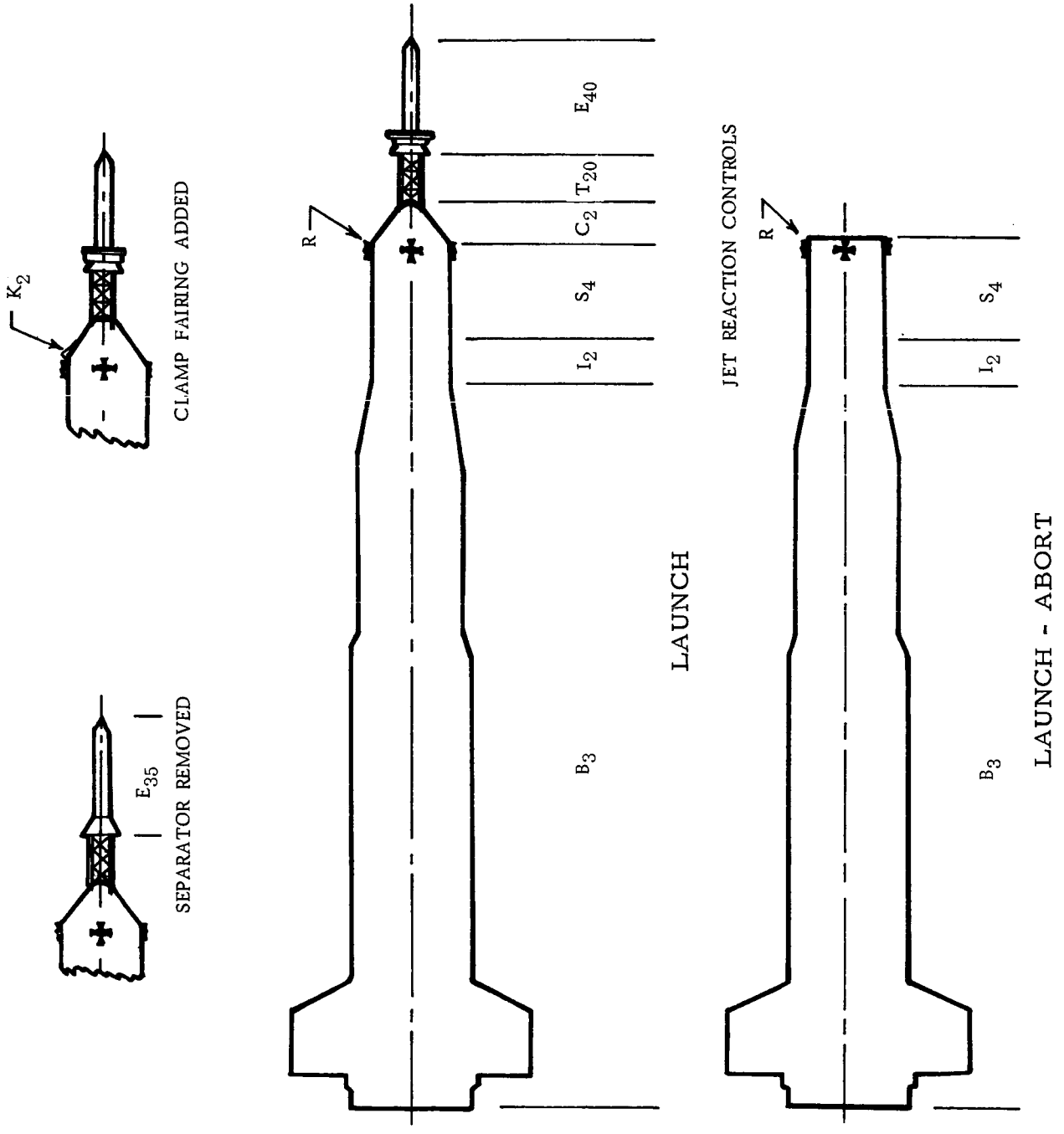

Figure 1. Test Configurations

CONFIDENTIAL

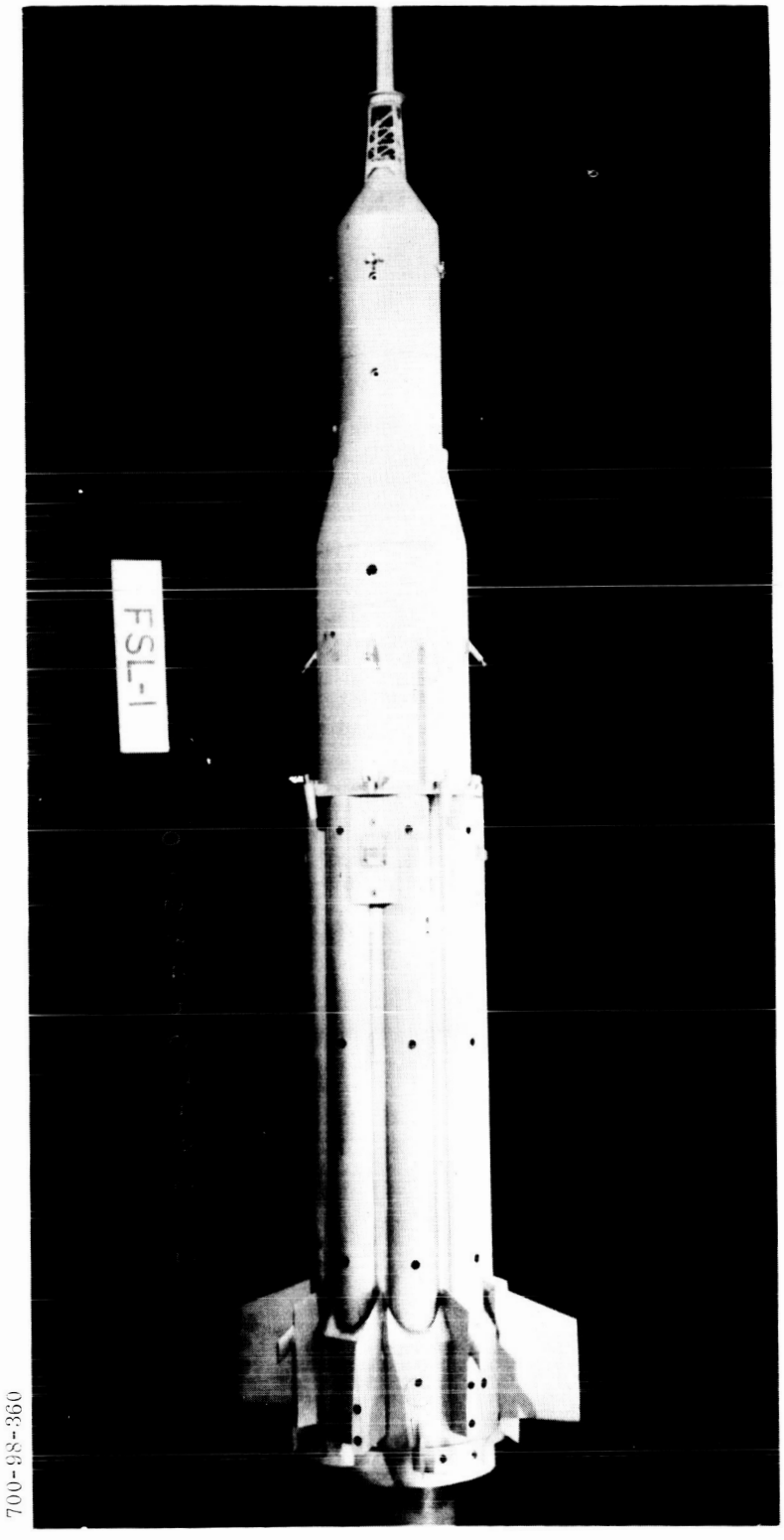

Figure 2. Launch Configuration

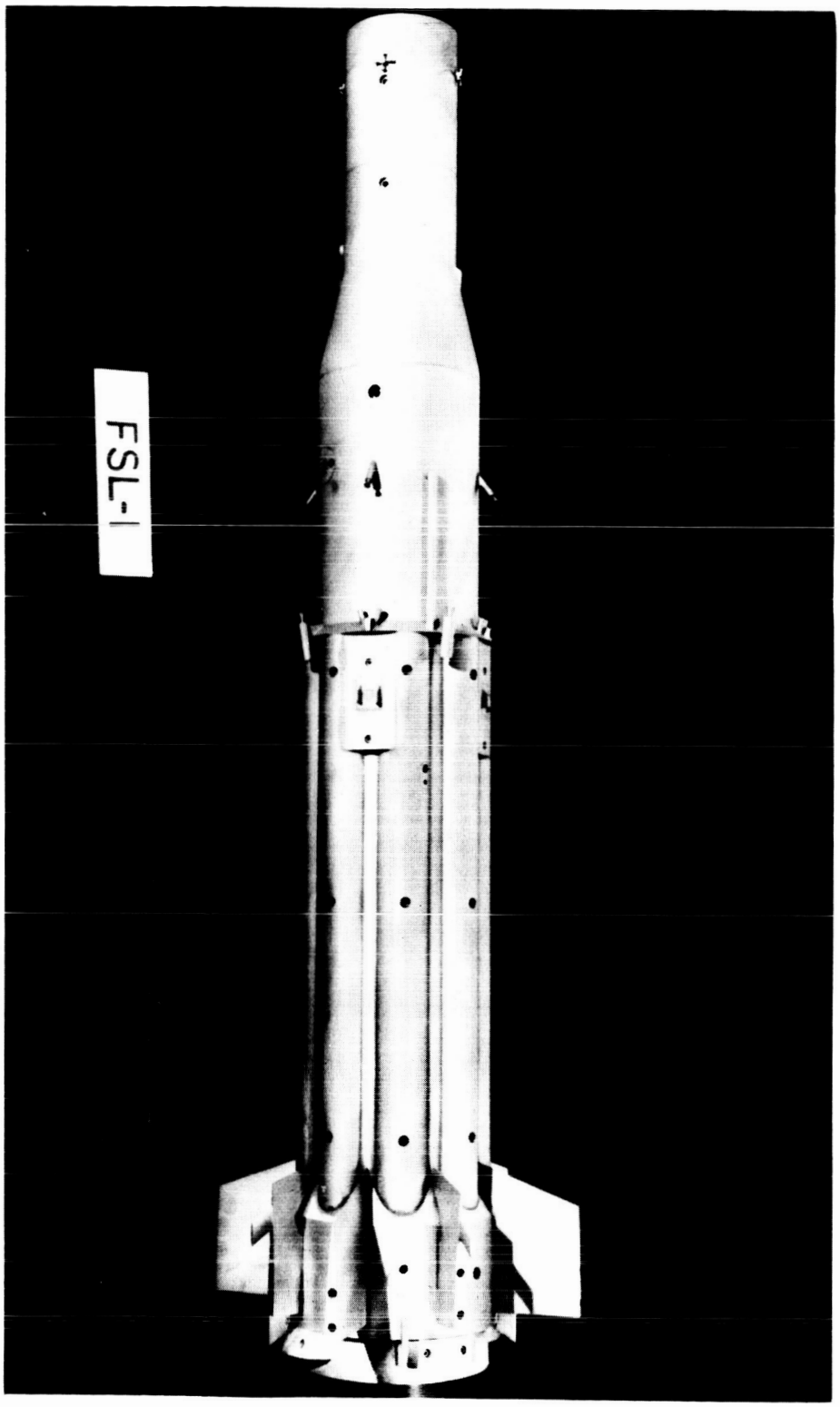

Figure 3. Launch-Abort Configuration

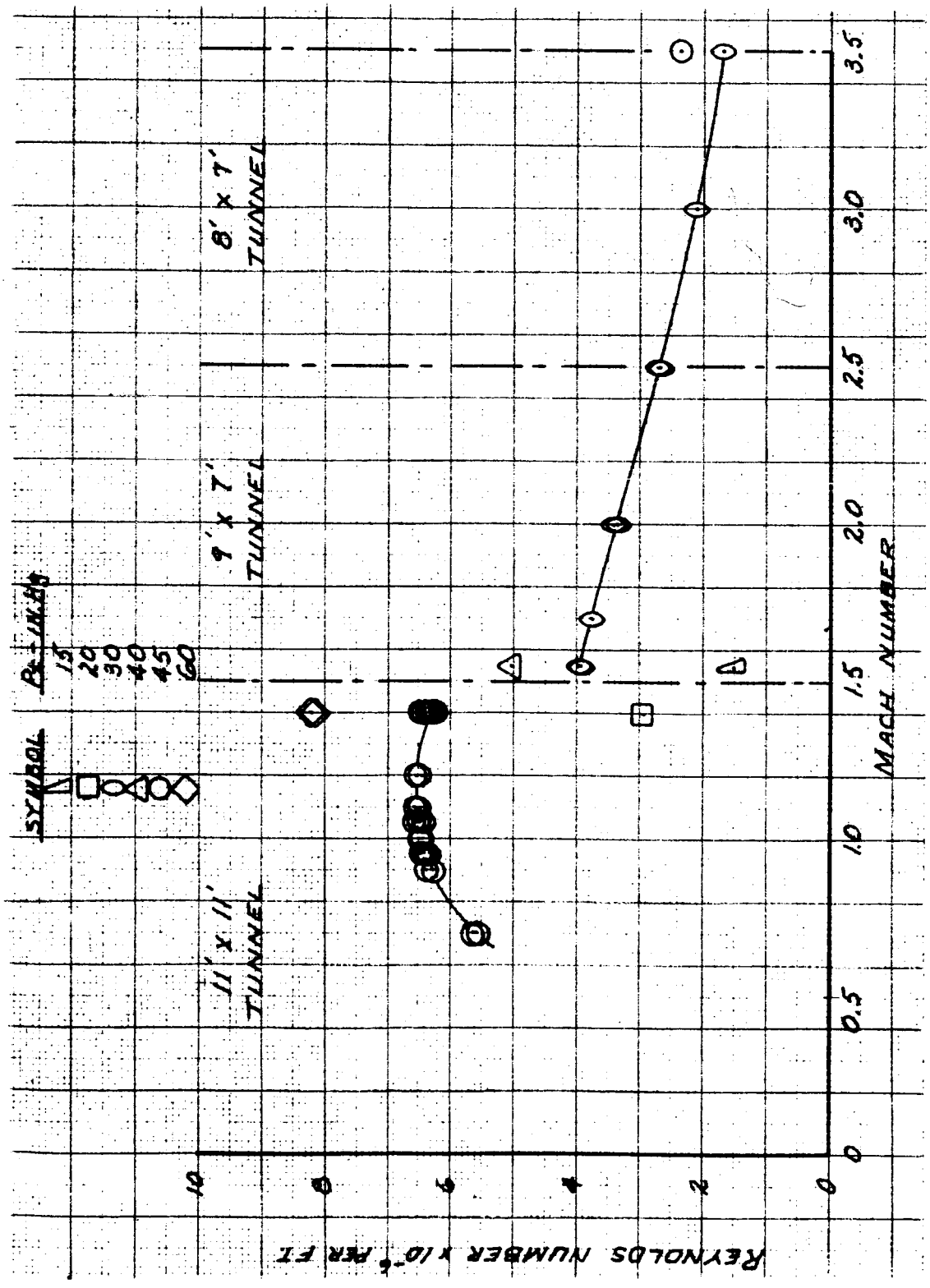

Figure 4. Variation of Reynolds Number with Mach Number

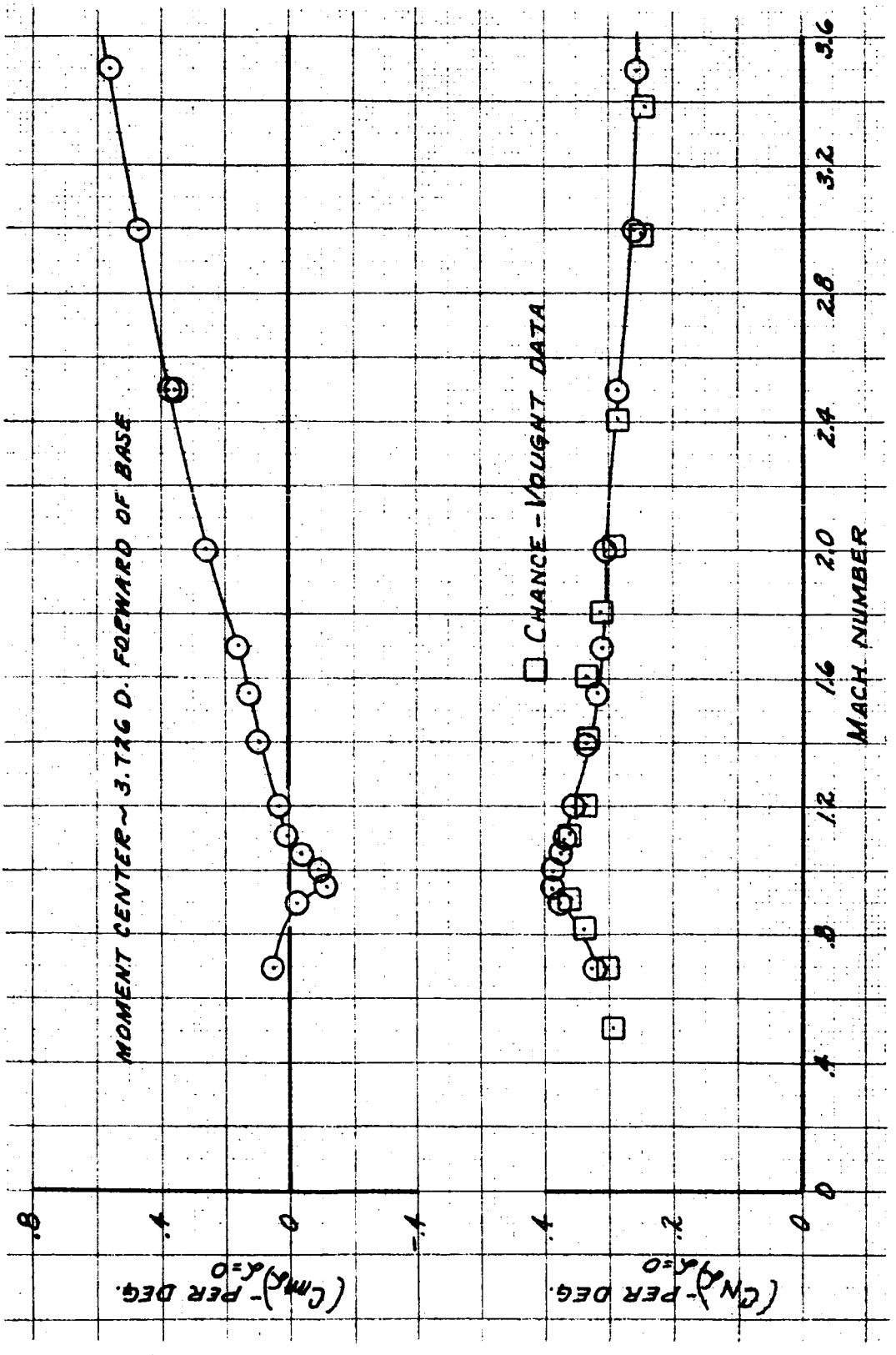

Figure 5. Effect of Mach Number on the Aerodynamic Coefficients for the Launch Configuration (Sheet 1 of 3)

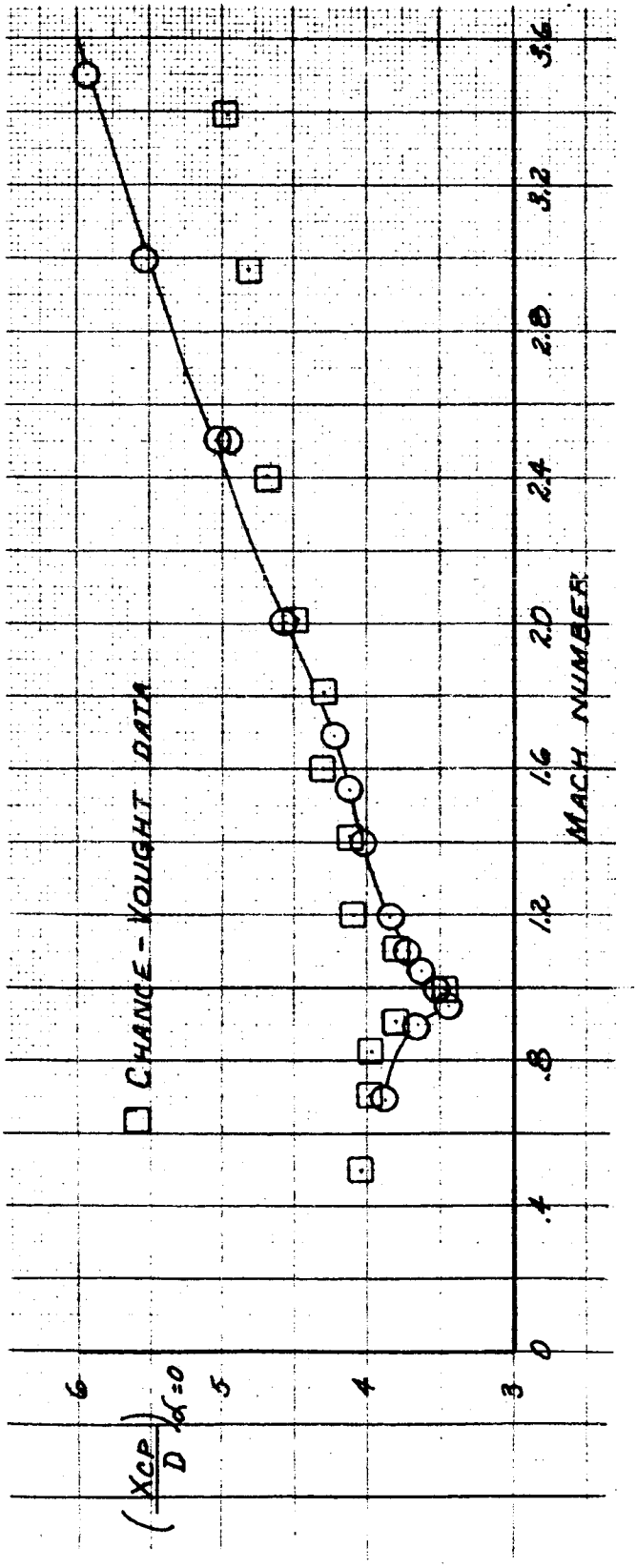

Figure 5. Effect of Mach Number on the Aerodynamic Coefficients for the Launch Configuration (Sheet 2 of 3)

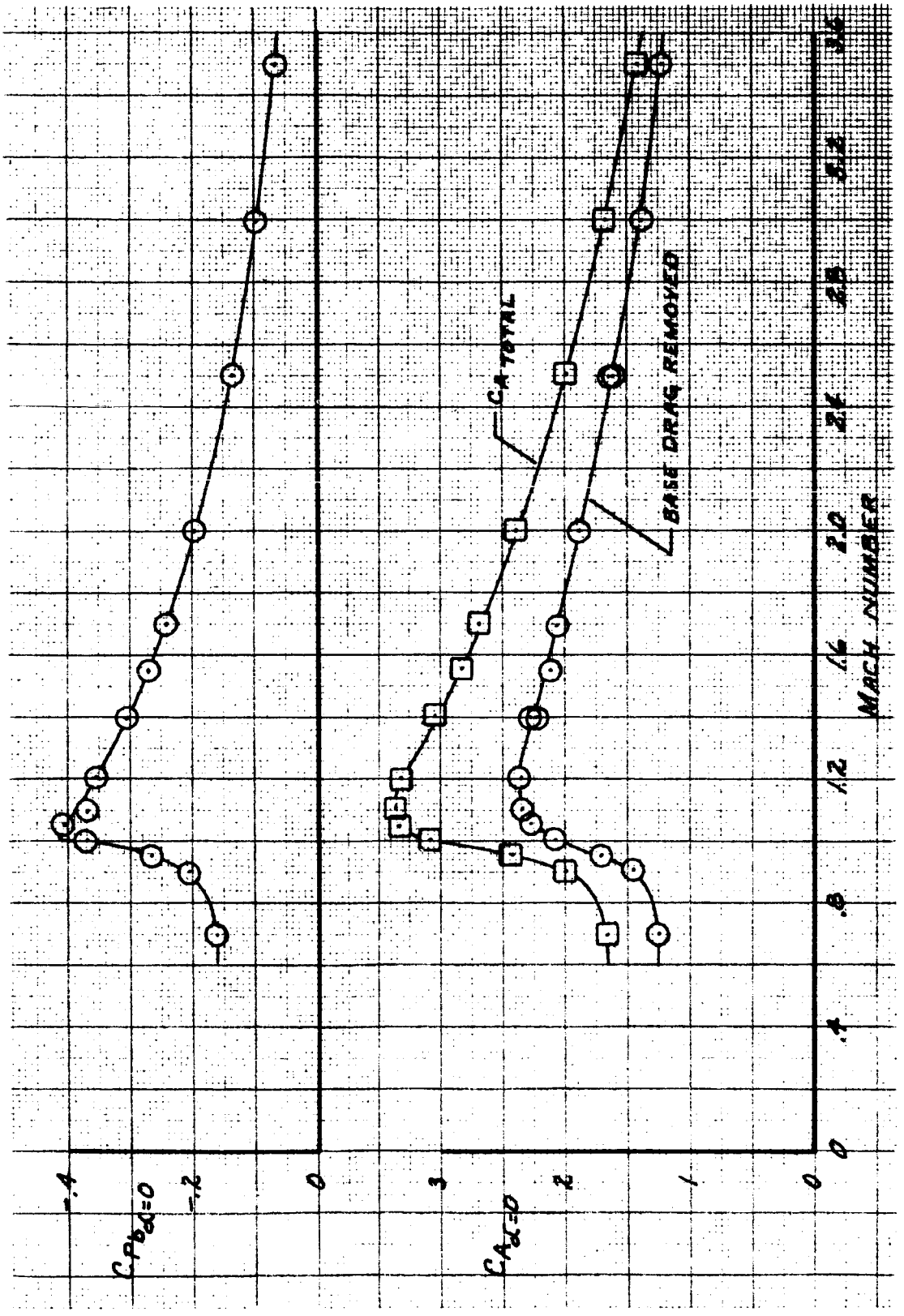

Figure 5. Effect of Mach Number on the Aerodynamic Coefficients for the Launch Configuration (Sheet 3 of 3)

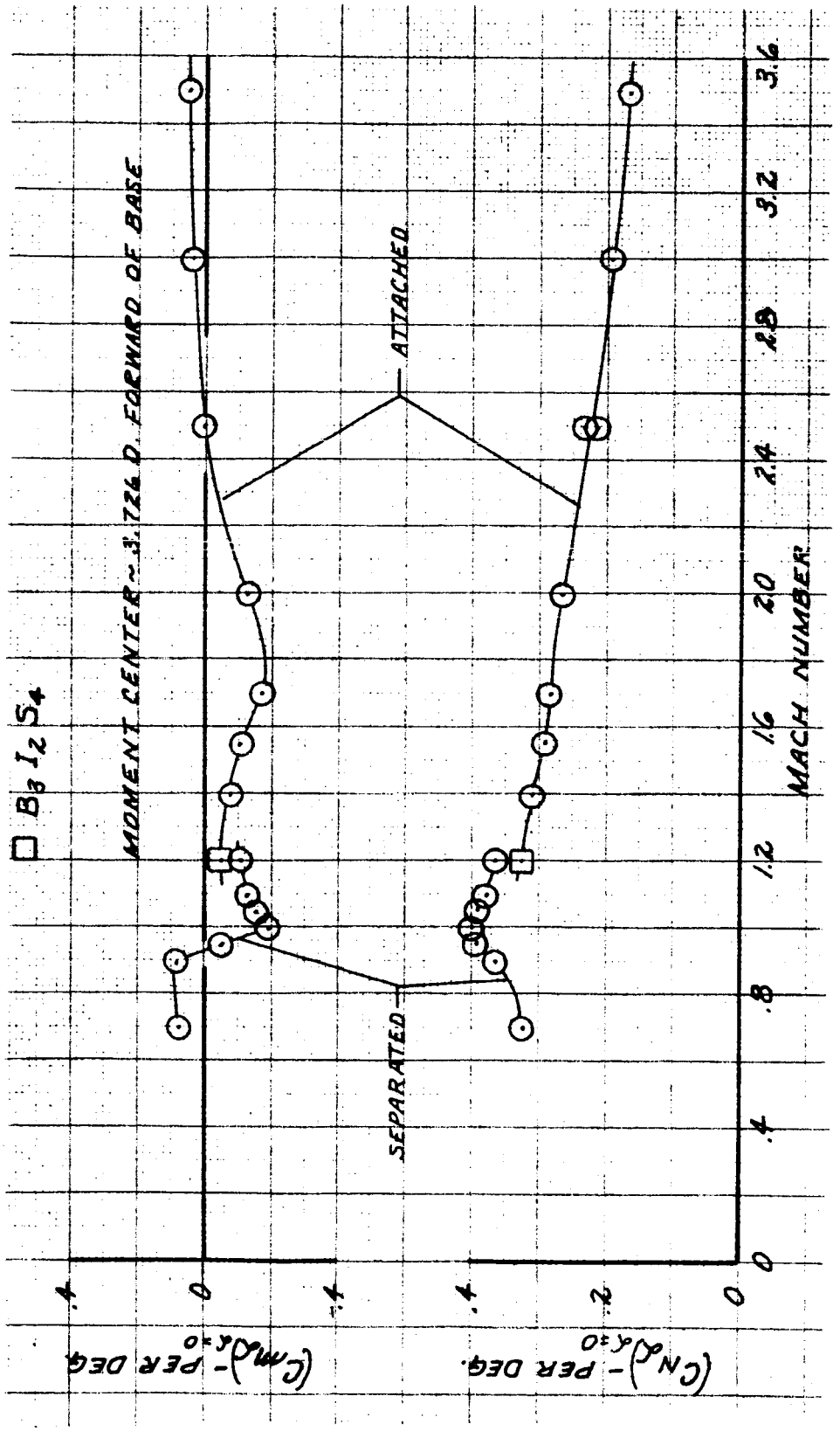

Figure 6. Effect of Mach Number on the Aerodynamic Coefficients for the Launch-Abort Configuration (Sheet 1 of 3)

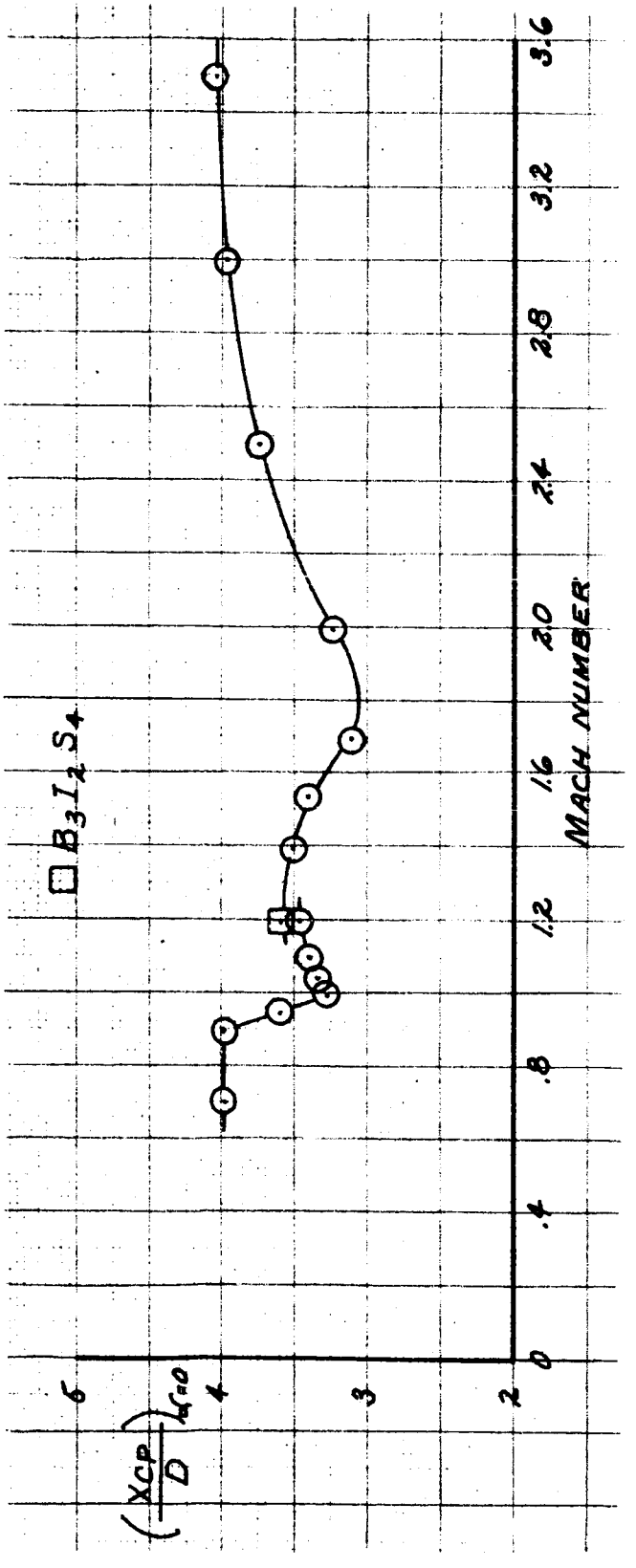

Figure 6. Effect of Mach Number on the Aerodynamic Coefficients for the Launch-Abort Configuration (Sheet 2 of 3)

CONFIDENTIAL

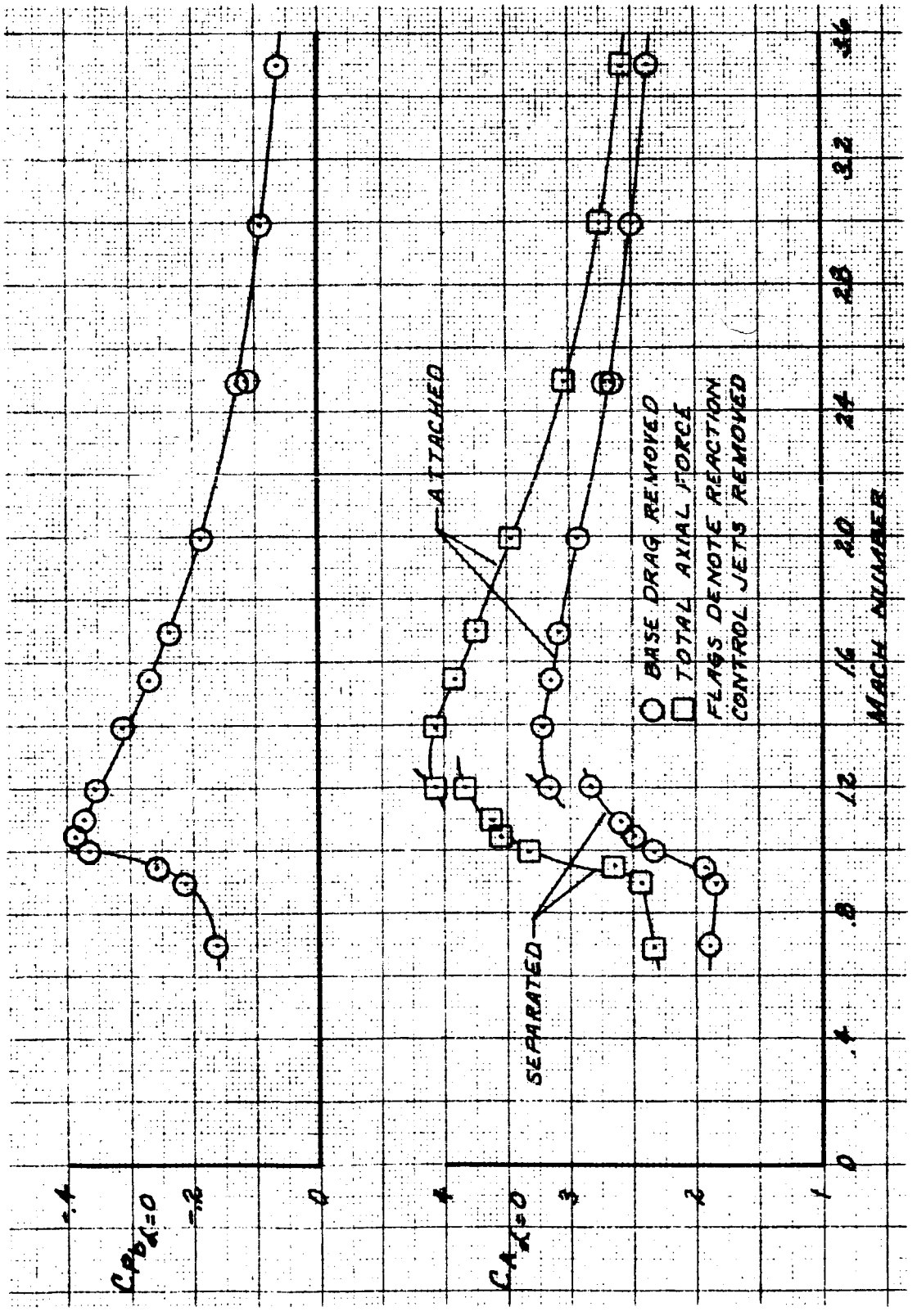

Figure 6. Effect of Mach Number on the Aerodynamic Coefficients for the Launch-Abort Configuration (Sheet 3 of 3)

CONFIDENTIAL

SEPARATED

ATTACHED

700-98-357

Figure 7. Schlieren Photographs of Attached and Separated Flow Fields at Mach Number 1.20

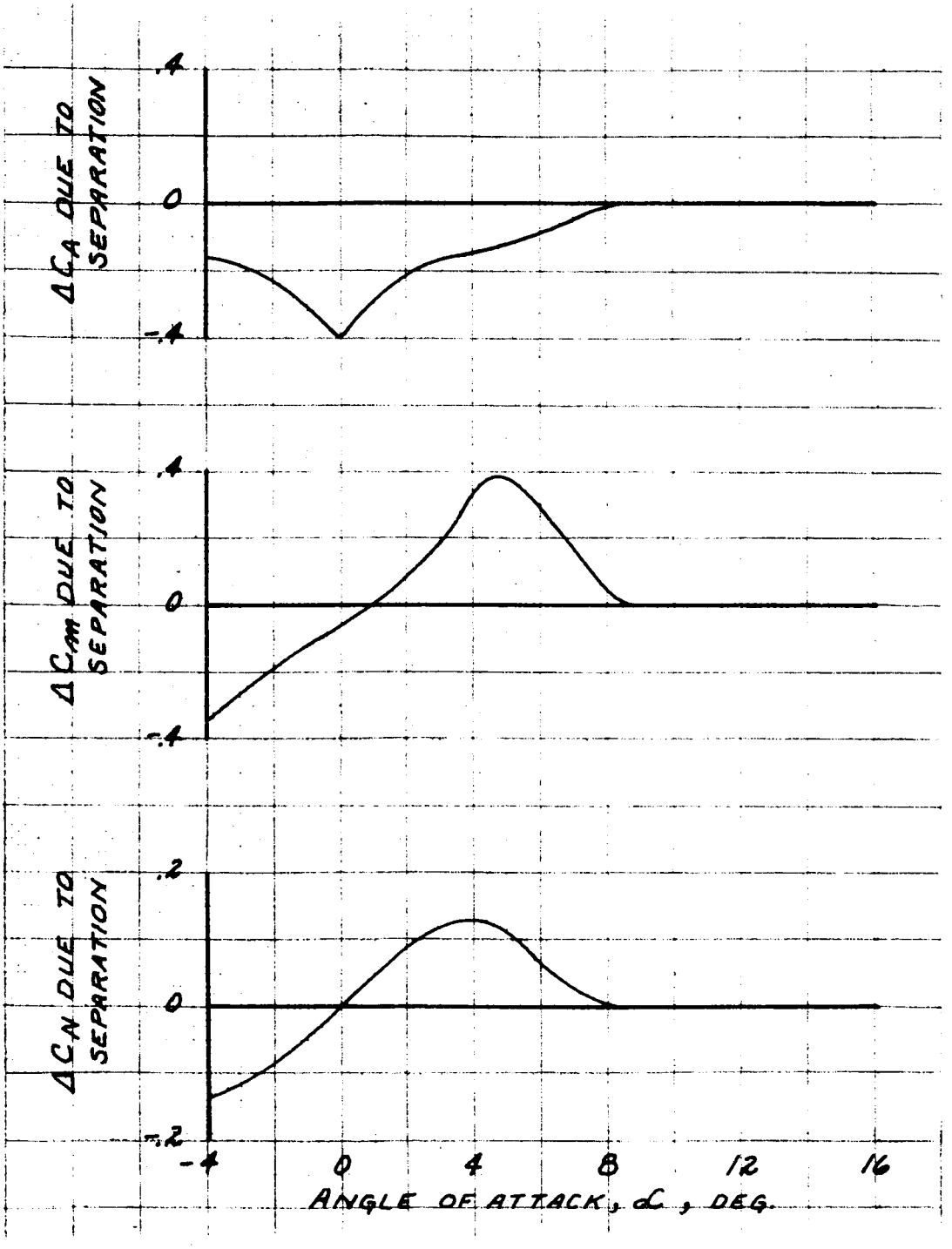

Figure 8. Effect of Separation at Mach Number 1.20 for Launch-Abort Configuration

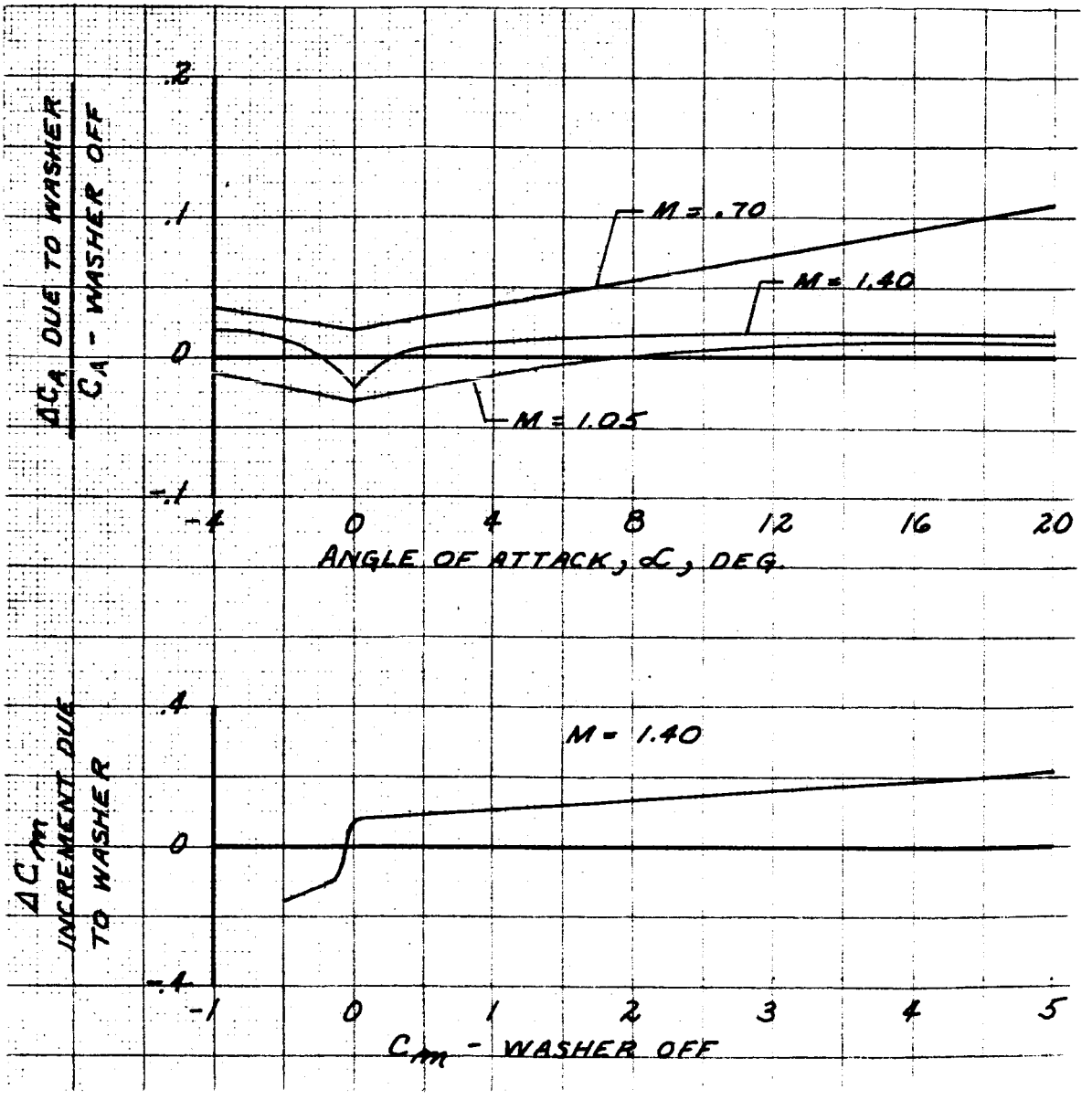

Figure 9. Effect of Launch Escape System Separator on Axial Force and Pitching Moment

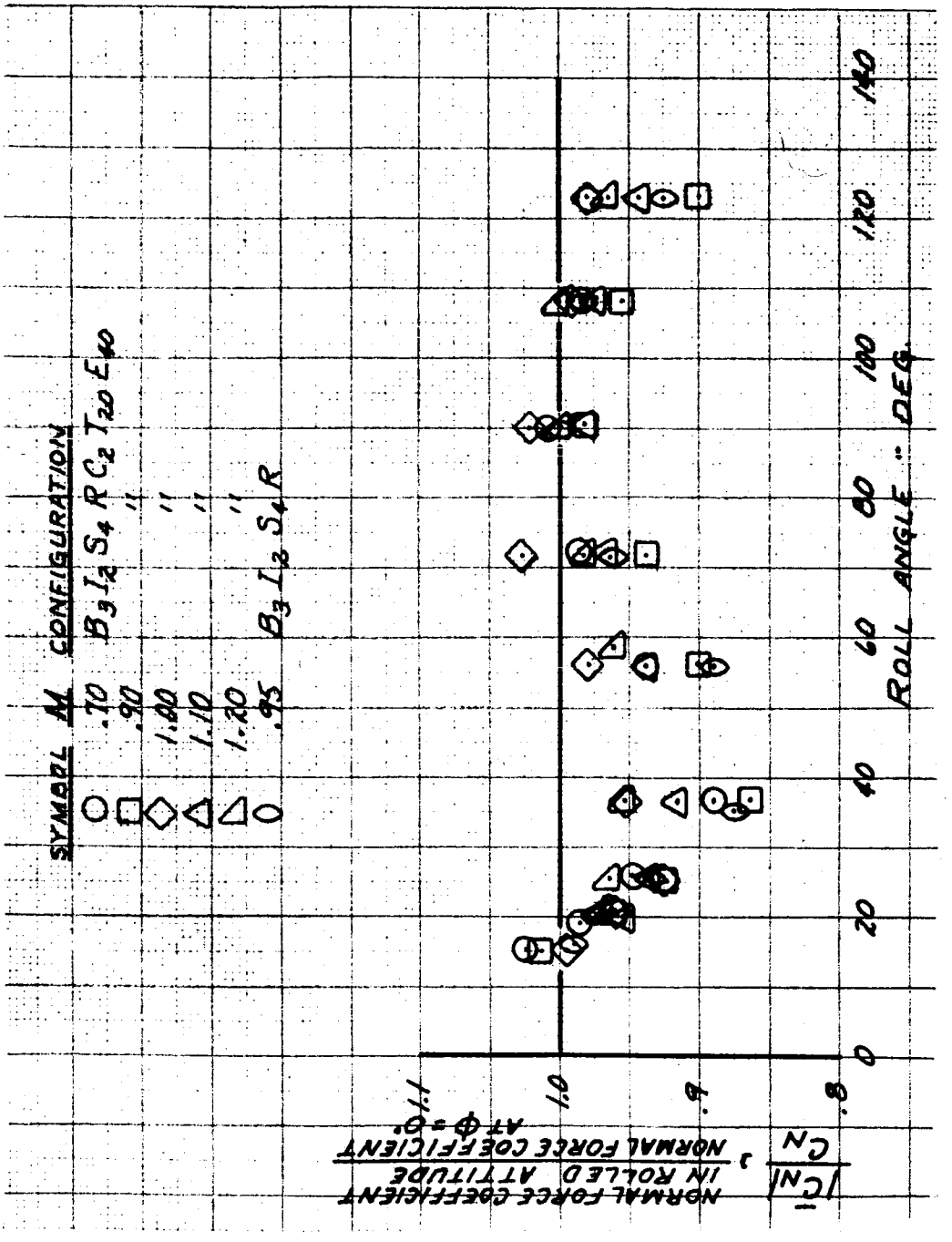

Figure 10. Effect of Roll Attitude on Normal Force Coefficient

CONFIDENTIAL

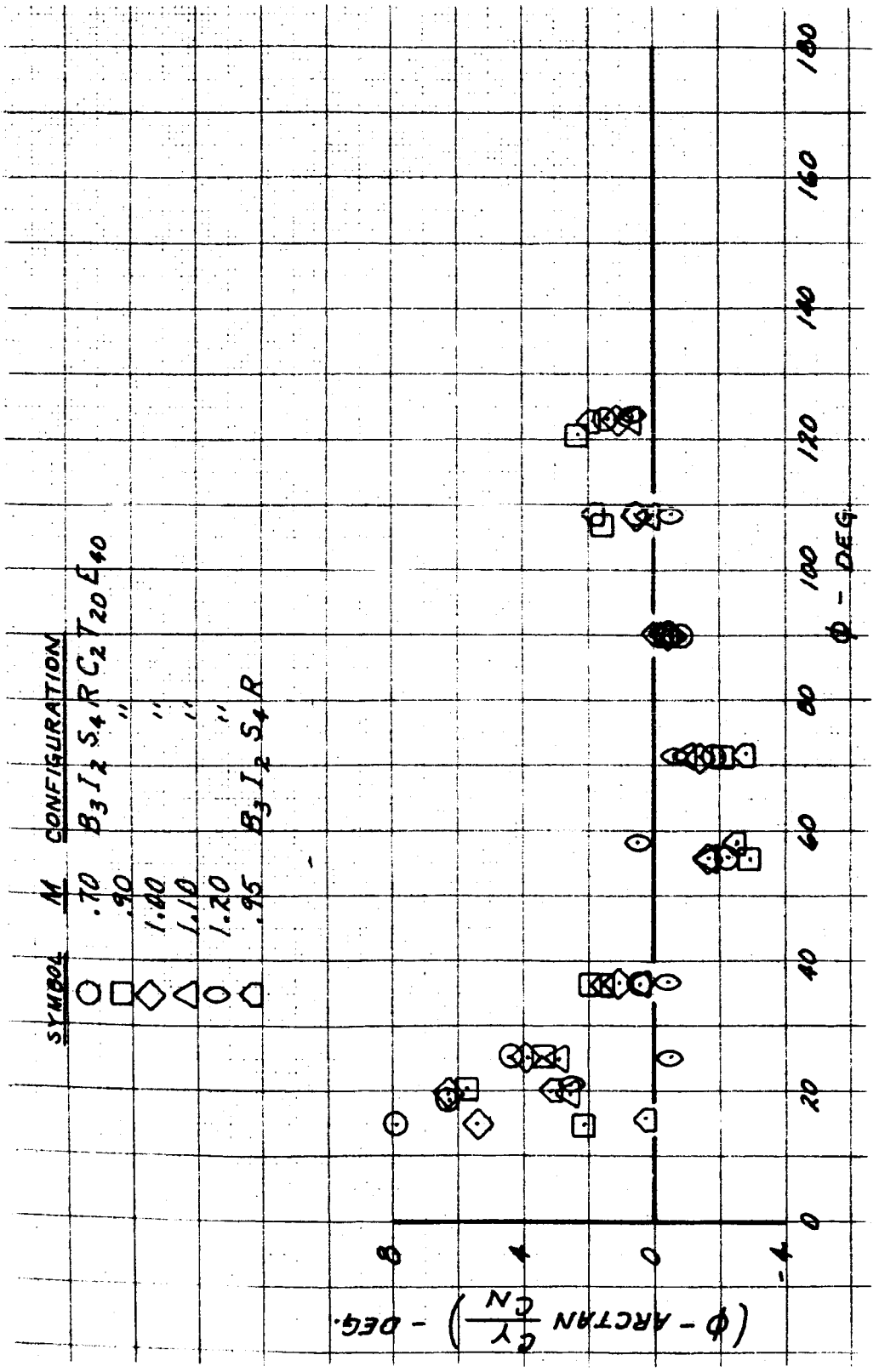

Figure 11. Effect of Roll Attitude on Inclination of Composite Normal Force Coefficient

CONFIDENTIAL

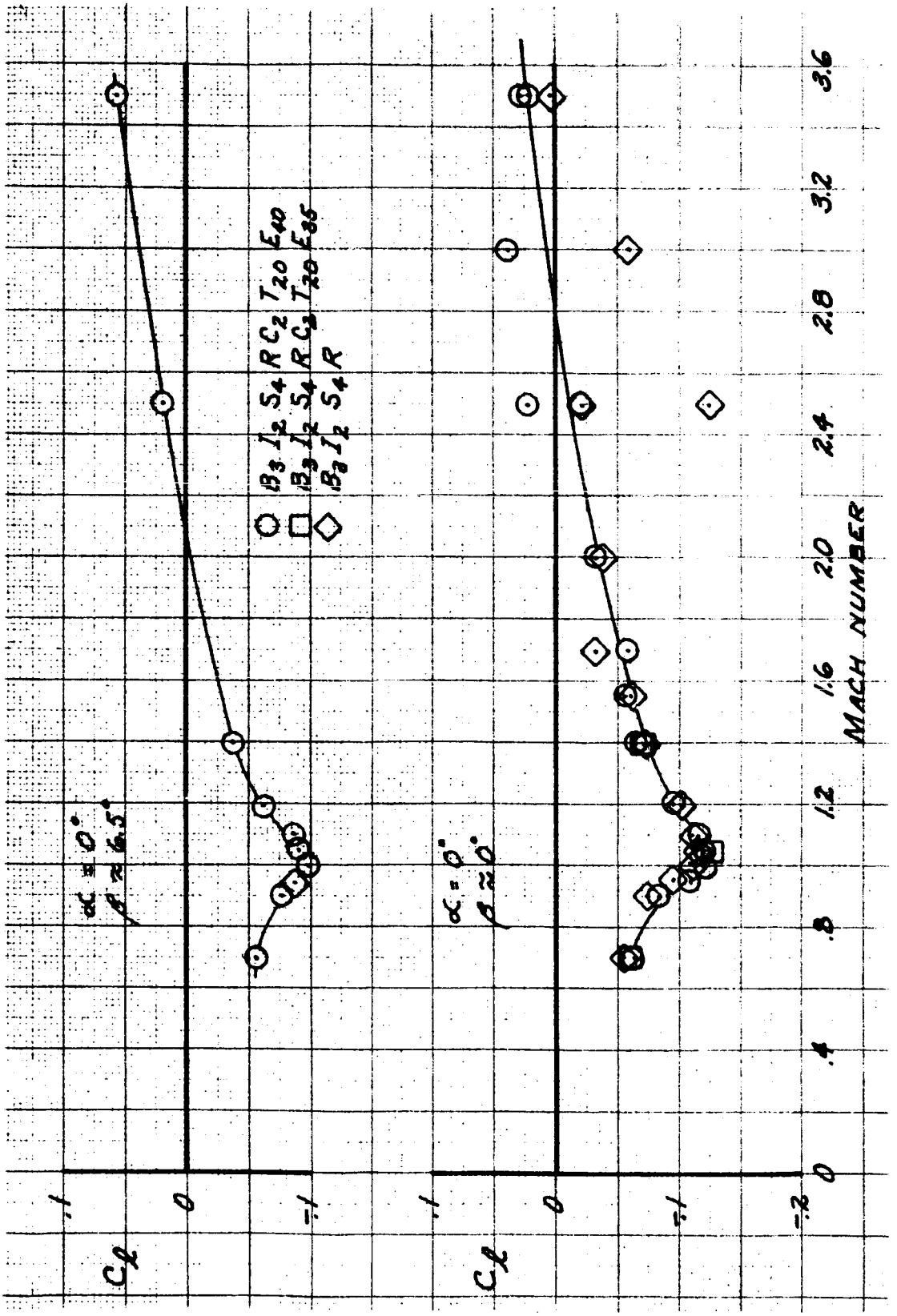

Figure 12. Effect of Mach Number on Rolling Moment Coefficient at β = 0 and 6.5 Degrees

CONFIDENTIAL

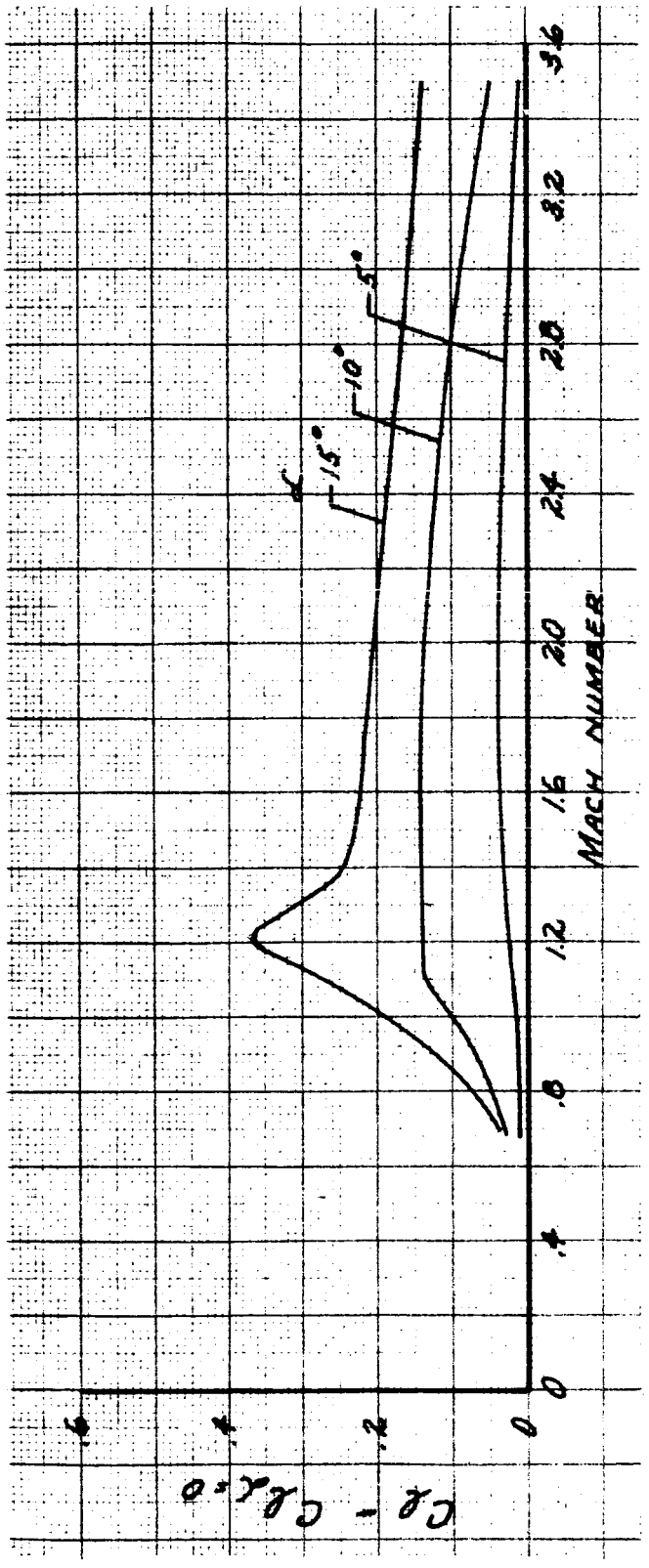

Figure 13. Effect of Mach Number on the Increment of Rolling Moment Coefficient Due to Angle of Attack at $\beta = 6.5$

CONFIDENTIAL

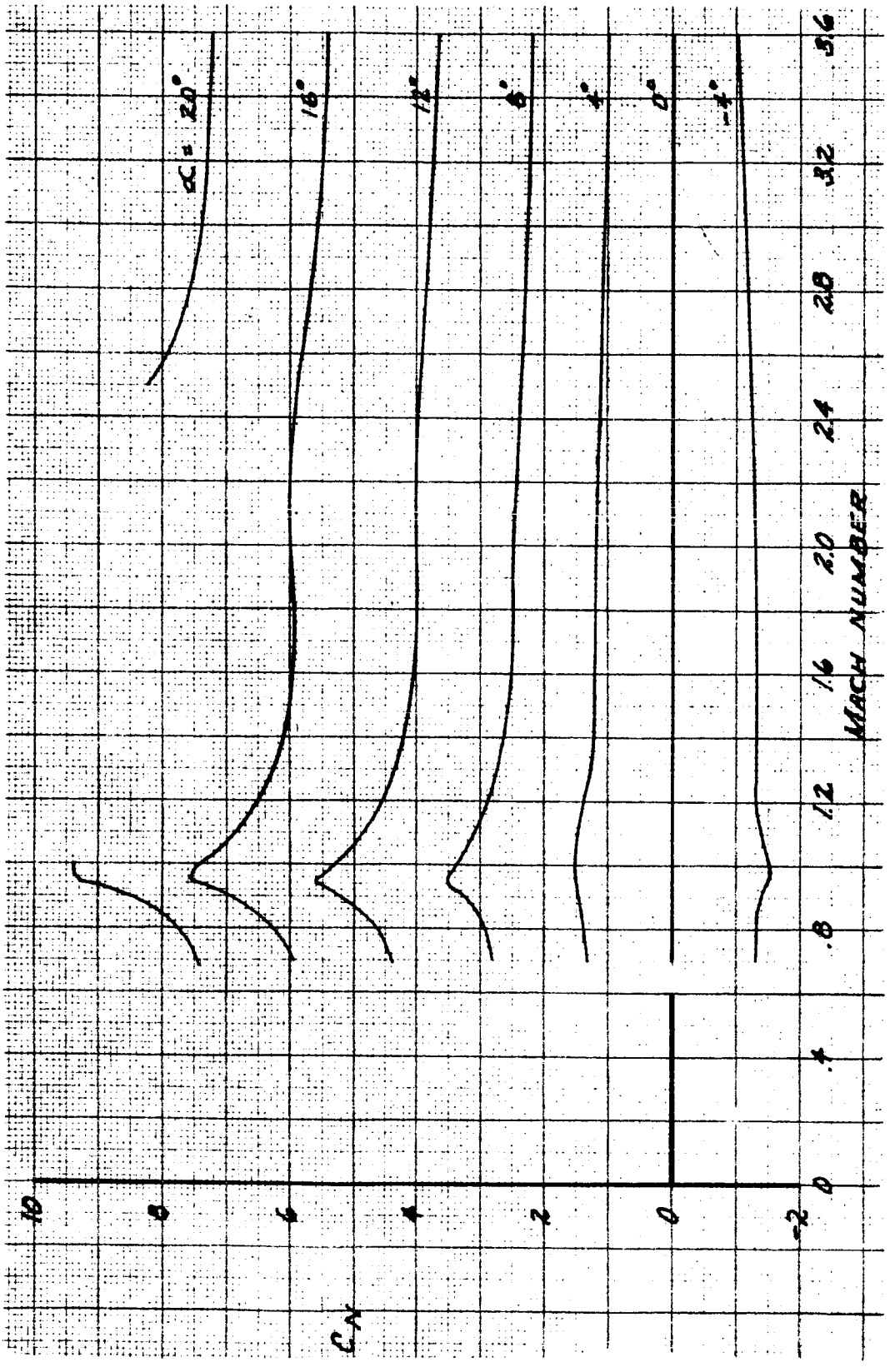

Figure 14. Effect of Mach Number on Aerodynamic Coefficients at Angles of Attack for the Launch Configuration (Sheet 1 of 3)

~~CONFIDENTIAL~~

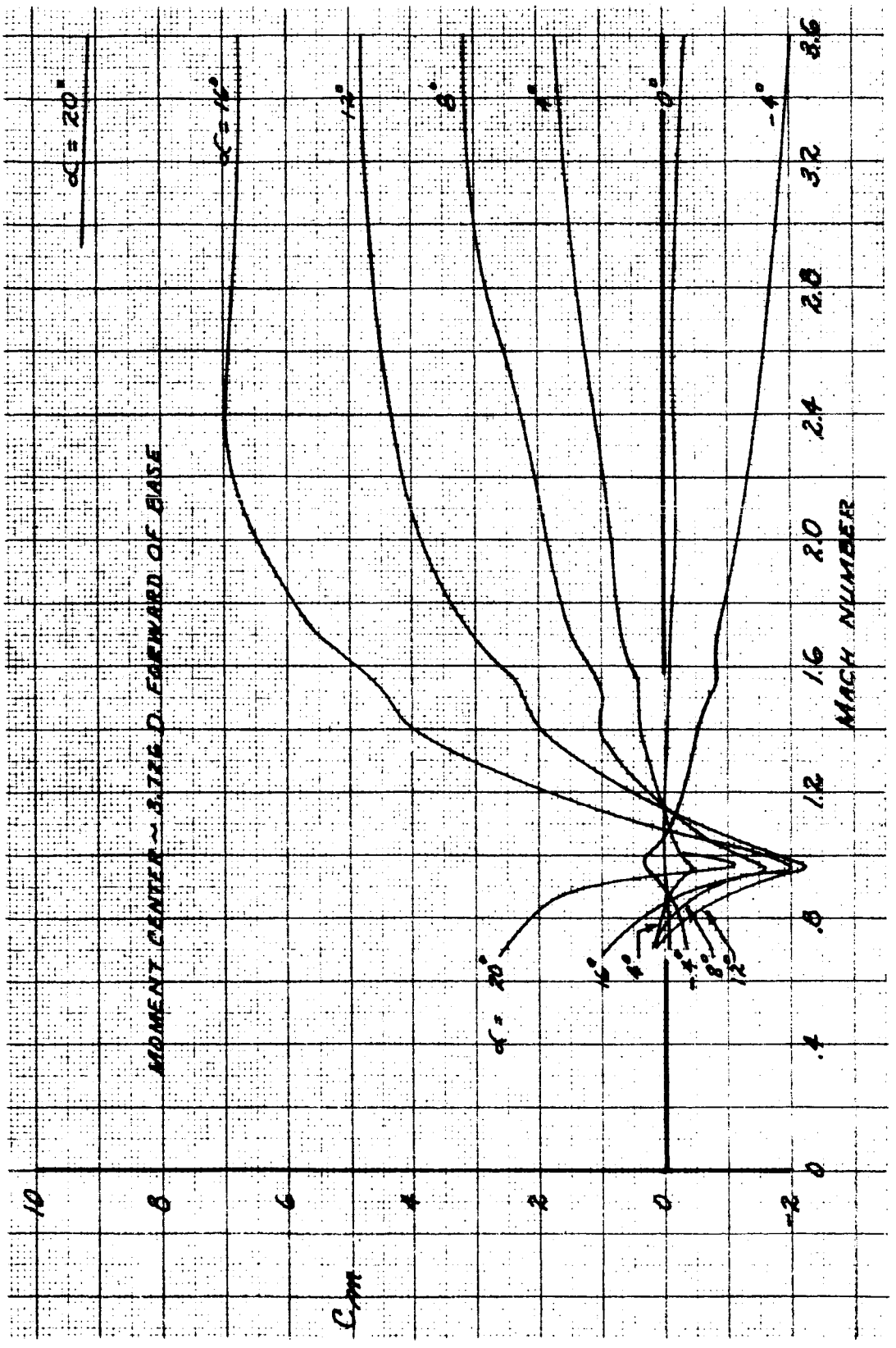

Figure 14. Effect of Mach Number on Aerodynamic Coefficients at Angles of Attack for the Launch Configuration (Sheet 2 of 3)

~~CONFIDENTIAL~~

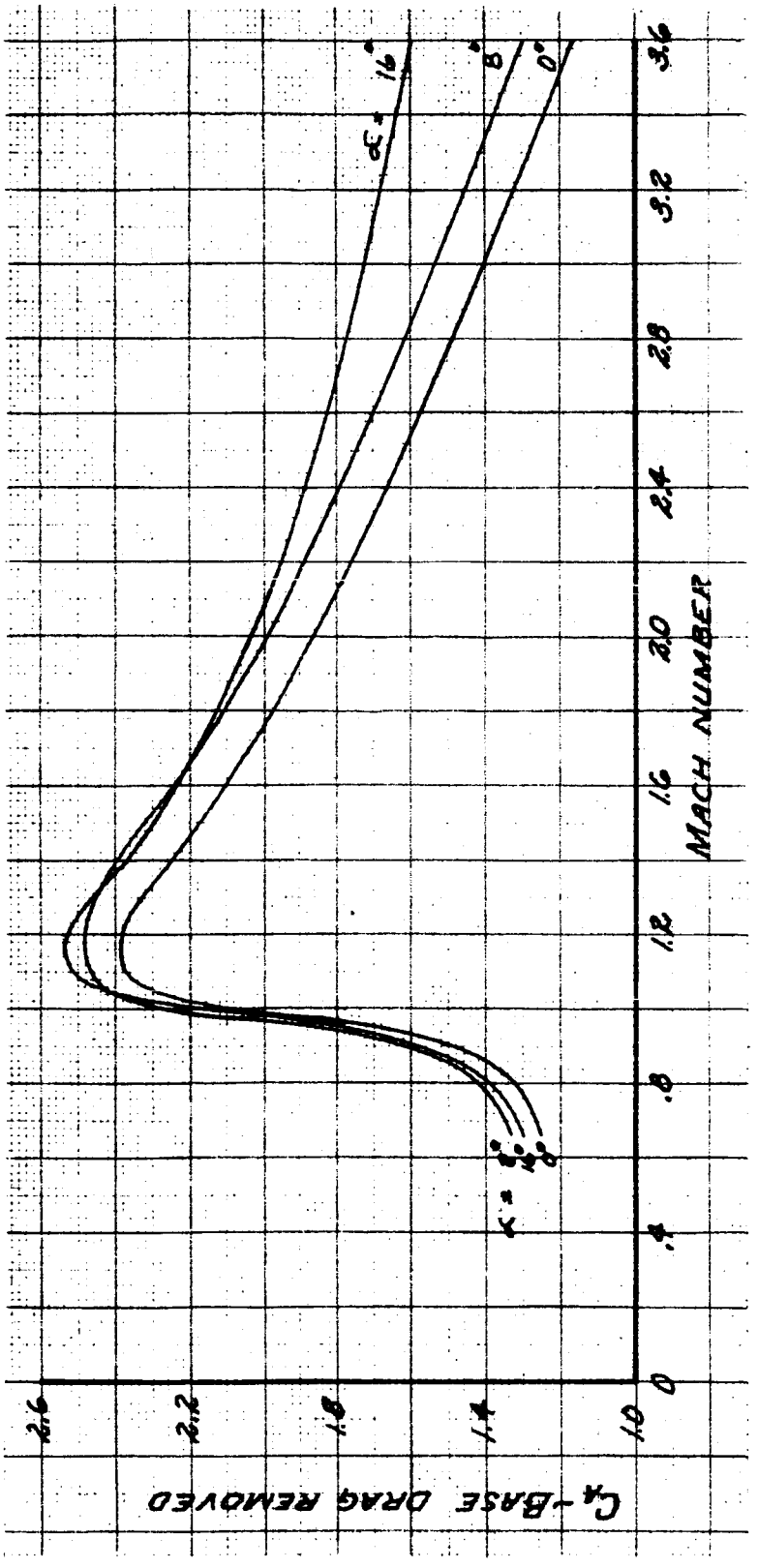

Figure 14. Effect of Mach Number on Aerodynamic Coefficients at Angles of Attack for the Launch Configuration (Sheet 3 of 3)

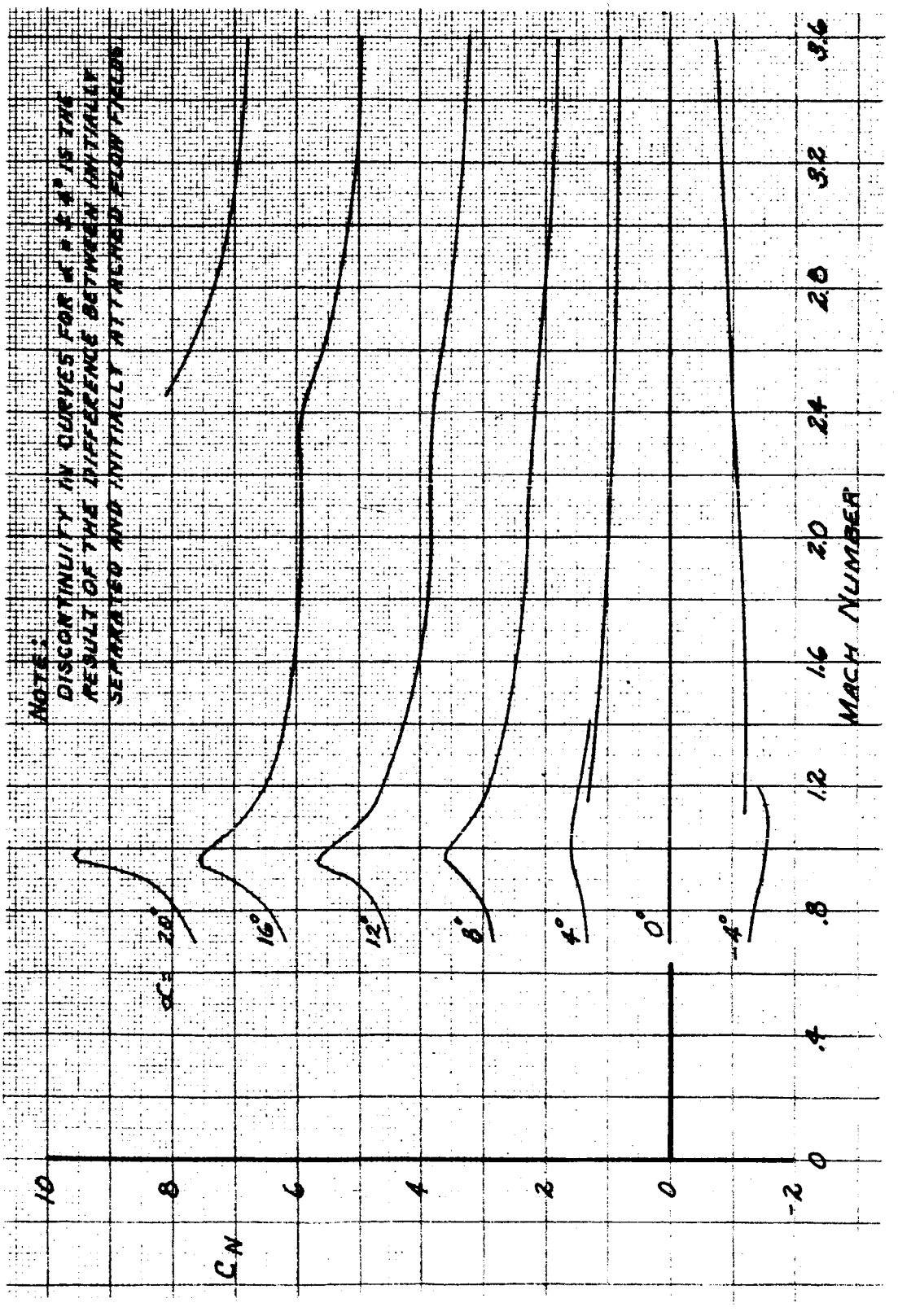

Figure 15. Effect of Mach Number on Aerodynamic Coefficients at Angles of Attack for the Launch-Abort Configuration (Sheet 1 of 3)

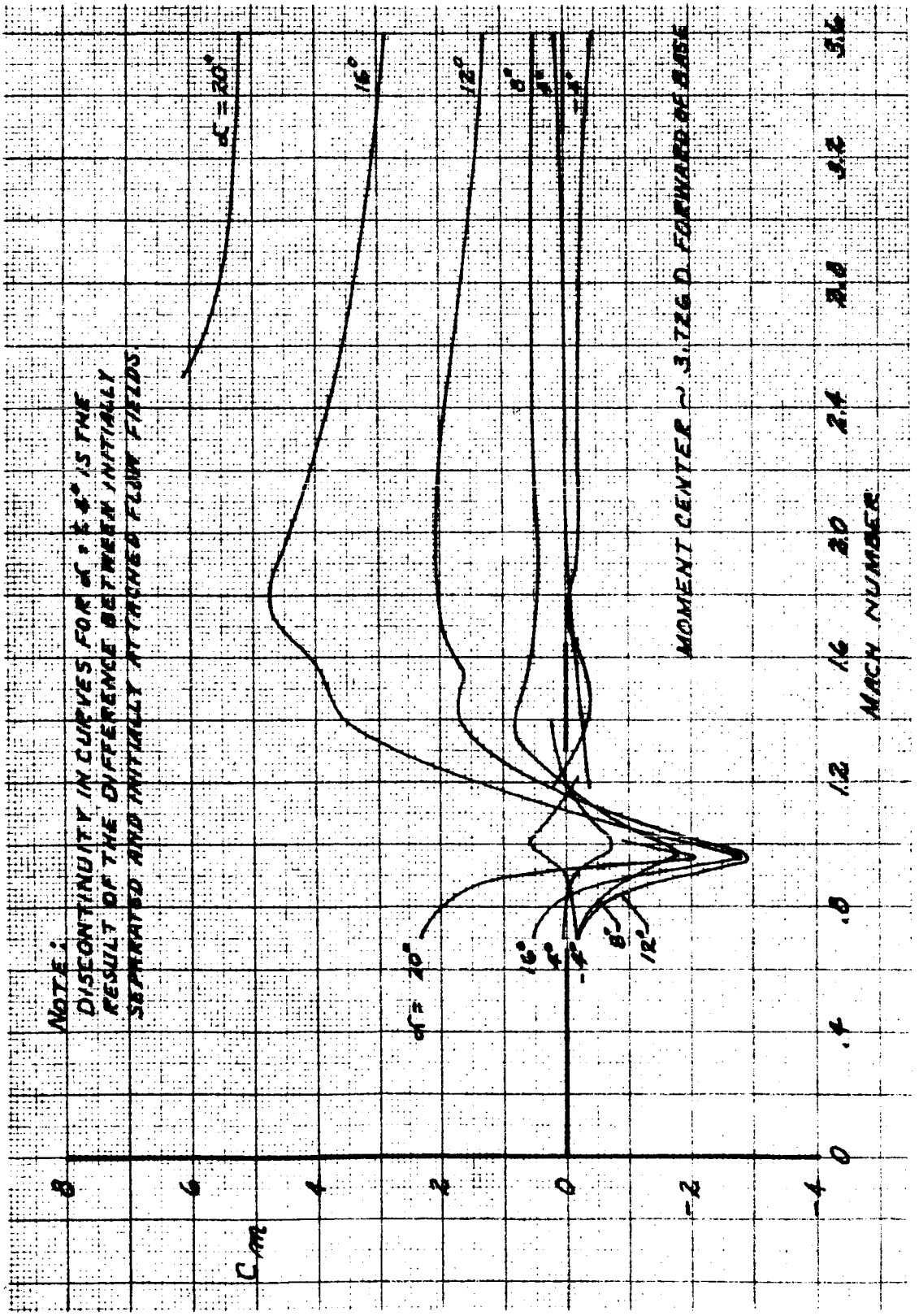

Figure 15. Effect of Mach Number on Aerodynamic Coefficients at Angles of Attack for the Launch-Abort Configuration (Sheet 2 of 3)

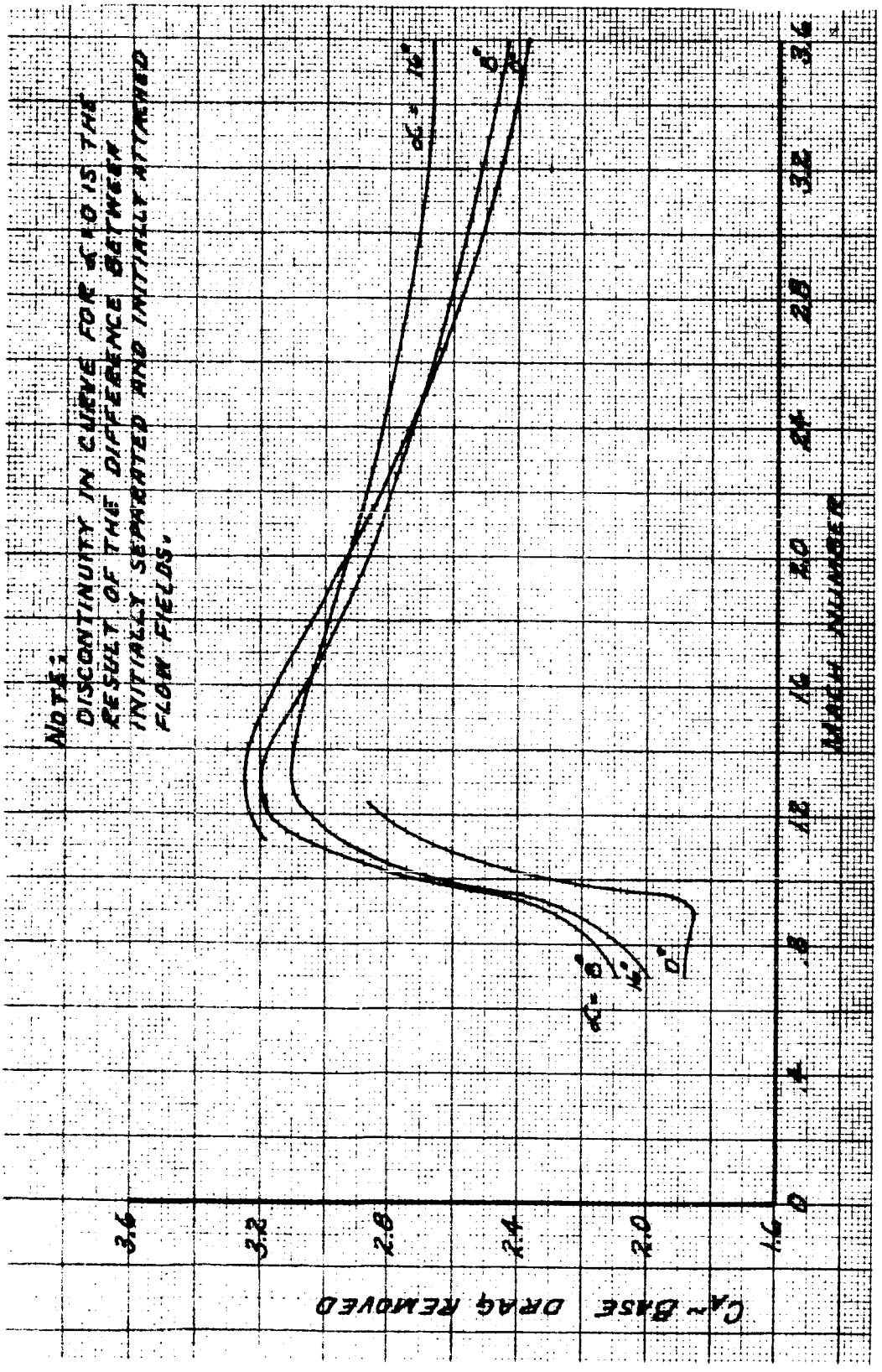

Figure 15. Effect of Mach Number on Aerodynamic Coefficients at Angles of Attach for the Launch-Abort Configuration (Sheet 3 of 3)